HERON is jointly edited by:
STEVIN-LABORATORY of the faculty of Civil Engineering, Delft University of Technology, Delft, The Netherlands
and
TNO BUILDING AND CONSTRUCTION RESEARCH. Rijswijk (ZH), The Netherlands
HERON contains contributions based mainly on research work performed in these laboratories on strength of materials, structures and materials science.

ISSN 0046-7316

Secretary:
J. G. M. van Mier
Stevinweg 1
P.O. Box 5048
2600 GA Delft, The Netherlands
Tel. 0031-15-784578
Fax 0031-15-611465
Telex 38151 BUTUD

HERON vol. 38 1993 no. 1

Contents

MICROSTRUCTURE OF THE INTERFACIAL ZONE AROUND AGGREGATE PARTICLES IN CONCRETE

J. A. Larbi
TNO Building and Construction Research
Department of Building Technology
Rijswijk

Publication in HERON since 1970

Preface

This publication is based on the doctors thesis of the author which was carried out at Delft Technical University, Faculty of Civil Engineering, Materials Science Group from 1987 to 1991. It deals with a study about the microstructure of the cement paste-aggregate interfacial zone in concrete.
The study is aimed at: (i) examining the microstructural characteristics of the interfacial region around aggregate particles in concrete and (ii) exploring the influence of this interfacial zone on some of the properties of concrete such as, the compressive strength, the water transport capacity, and the diffusion of ions into concretes prepared with and without mineral additives.

Microstructure of the Interfacial Zone around Aggregate Particles in Concrete

1 Introduction and Literature Review

1.1 *General*

Concrete may be modelled to consist of cement paste, pore water and inserts. The inserts may be aggregate particles or fillers, fly ash particles or other pozzolanic materials, reinforcements, and fibres of steel, glass, or natural and synthetic organic materials. As such, different types of interfaces between the inserts and the cement paste may exist.

There is ample evidence that the properties of concrete such as the compressive strength, the tensile strength, the bond strength, modes of failure, the bending stiffness and the permeability are significantly influenced by the nature of interfaces existing between the cement matrix and the inserts. For this reason, the paste-insert interfacial zone is regarded as a weak link in concrete. Since the early eighties efforts aimed at improving the quality of this so-called weak interfacial regions around inserts in concrete, particularly, the cement paste-aggregate interfacial zone have been intensified. However, due to lack of understanding about these interfaces, most of the attempts that have been made to improve these interfaces have yielded relatively little fruitful results. At the moment, for instance, there is no simple method of predicting how much improvement can be made in the overall performance of concrete through improvements of the interfacial zone. The study presented in this publication is concerned only with the microstructure of the interfacial zone between cement paste and normalweight or conventionally used aggregate particles (crushed granite, crushed limestone, gravels and sands) in concrete. No lightweight aggregates were considered. In this publication, the terms "interfacial zone", "transition zone", "interfacial region", "transition region", "interfacial layer" and "transition layer", all refer to the same material, that is, the cement paste layer that is formed around aggregate particles in concrete. It is also worthwhile to mention that in all the mixes containing mineral additives, the latter were used as partial portland cement replacements (by mass). All the samples used were cured in water; drying-out of the samples was prevented as much as possible.

1.2 *Interfaces in Concrete*

In hardened concrete, a number of interfaces between cement paste and inserts may exist. These may be classified broadly into five groups as follows [1]:

a. interfaces between the various phases that make up the cement paste, including interfaces between the cement paste and the unhydrated or partially hydrated cement;

b. interfaces between the cement paste and the unreacted or partially reacted pozzolanic materials;
c. interfaces between the cement paste and aggregate particles;
d. interfaces between the cement paste and steel reinforcements;
e. interfaces between cement paste and fibres that may be present in special concretes.

In the sections that follow, a review of the microstructural features of interfacial zone around aggregate particles and their influences on the strength and the durability of portland cement composites are presented. As mentioned already, the work reported here concerns only interfaces and bonding between cement pastes and normalweight aggregate particles. Not considered in depth are interfaces and bonding in particulate materials or phases within cement pastes such as, (a) intraparticle bonding involving interatomic forces within individual hydration products, such as those within C–S–H or $Ca(OH)_2$, and (b) interparticle bonds, involving atomic forces which bond the individual particles to each other and to grains of the anhydrous cement. Also interfacial morphologies between cement pastes and continuous and discontinuous reinforcements (iv and v above) will not be discussed.

1.3 *Microstructure of the Cement Paste-Aggregate Interfacial Zone*

During mixing, placement and compaction of concrete, the aggregate particles interact with the surrounding cement paste. As a result, the microstructure of the cement paste at the immediate vicinity of aggregate particles becomes affected and tends to differ in several respects from the microstructure of the bulk cement matrix. In this section, the microstructural characteristics of the cement paste-aggregate interfacial zone is reviewed in relation to the present study.

One of the first workers to study the microstructure of the paste-aggregate interfacial zone was Farran [2]. He examined the nature of the bond between different types of minerals and portland cement pastes at normal temperatures. A summary of his observations are as follows:

(i) that the bond between calcite or dolomite and cement paste was stronger than that of other minerals;
(ii) that the bond strength with fine-grained calcite was better than that with coarse-grained calcite rock;
(iii) that "corrosion" of calcite surfaces in contact with the cement paste occurred.

He found the paste-calcite bond strength to be higher than the rest of the minerals examined and concluded that this effect was due to the "corrosion" of the calcite surfaces. He explained that the "corrosion" was brought about by a slight dissolution of the calcite surfaces with subsequent "epitaxial" formation of calcium hydroxide-calcite solid solution. This product, according to him, formed a "bridge" across the paste-calcite interface which increased the bond strength.

Buck and Dolch [3] performed a similar study but on a more elaborate scale using different minerals and aggregates. They reported similar observations to support the conclusions of Farran. They proposed that the reaction between the fine-grained, non-

dolomitic limestone and the portland cement paste was due to attack on the carbonate by alkali solutions in the cement paste. Some of the calcite, according to them, "transformed" into calcium hydroxide, which precipitated with a definite orientation at the rock-paste interface.

The results of the investigations carried out by Farran [2] and Buck and Dolch [3] indicate that at the interfacial zone between cement paste and calcareous aggregates, a kind of chemical reaction occurs in which calcium hydroxide is produced with a definite orientation to the aggregate surface.

Using a scanning electron microscope (SEM), Suzuki and Mizukama [4,5] studied the microstructure of the cement hydration products at the paste-aggregate interfacial zone. They observed that on each rock type, various phases of cement hydration products formed. But the crystallinity and the amount of hydrates formed varied from one type of aggregate to the other.

A more intriguing characteristic of the paste-aggregate interfacial zone was presented by Hadley [6], and later by Barnes et al. [7, 8]. They used a SEM equipped with an energy dispersive X-ray analyzer (EDAX) to study the micromorphology of the interfacial zone. Glass and α-quartz granules were used as model "coarse aggregates". With the aid of the EDAX facility, they were able to estimate the chemical composition of the hydration products in the interfacial zone. They reported the formation of a continuous film of cement hydrates predominantly calcium hydroxide $Ca(OH)_2$, intermixed with C–S–H (see Appendix for list of symbols and definitions) and ettringite as a deposition on the glass and quartz surfaces.

Initially, their method of study received some criticisms because the glass and α-quartz "aggregates" used for the studies were considered to be unrepresentative of conventionally used aggregates. For that matter, their interpretations were regarded as non-applicable to typical concrete systems. However, since their report, evidence from a number of studies involving cement paste-aggregate interfaces in typical concrete systems have supported their interpretations [9–12].

The microstructure of the interfacial zone which was modelled by Barnes et al. [7, 8] has been presented in detail by Diamond [13] as follows:

- in the immediate vicinity of the aggregate surface a "duplex film" of $Ca(OH)_2$ exists that is occassionaly intermixed with C–S–H; sometimes this duplex film occurs in close intimacy with the aggregate; at early ages of hydration, this duplex film is relatively porous; with increase in age, the film modifies into a dense layer, sometimes bonding with the surrounding cement paste; the side of the film in contact with the aggregate is a layer of crystalline $Ca(OH)_2$, ≈ 0.5 μm thick; following this layer is a thin deposit of C–S–H gel, in the form of short fibres, that extend into the cement paste; the total extent of the duplex film is ≈ 1.0 μm;
- next to the "duplex film" is the "transition zone"; this region is relatively larger, ≈ 50 μm wide, including the "duplex film"; generally, this zone contains a large number of hollow-shell hydration grains [6–8], and enriched in larger $Ca(OH)_2$ crystals and ettringite, AF_t.

The occurrence of a large number of hollow-shell hydration grains (consisting of only hydration products without unreacted cement klinker) suggests that cement hydration is accelerated at the interfacial zone. This is presumably because of an availability of excess water at the vicinity of the aggregate particles. Also, since the growth of large crystals of calcium hydroxide and ettringite is enhanced in a more open system, the occurrence of such large crystals at the interfacial zone is an indication of the existence of higher porosity.

Besides the model presented by Hadley [6] and Barnes et al. [7, 8], the microstructure of the paste-aggregate interfacial region has also been characterized by Zimbelmann [14]. He performed a combination of tensile bond strength tests and SEM studies on debonded paste-rock composites at various ages. Following these studies, he presented a model of the microstructure of the interfacial zone as follows:

a. directly at the surface of the aggregate there is a dense layer $\approx$ 2–3 μm thick and composed essentially of $Ca(OH)_2$ covering a network of ettringite crystals; this layer may be equivalent to the "duplex film" found by Barnes [7, 8]; according to Zimbelmann, this layer is formed during the early ages of hydration, that is, up to about 10 hours old; after about 12 hours the $Ca(OH)_2$ forms a continuous closed layer which he referred to as the "contact layer";
b. directly adjacent to the contact layer there is a zone $\approx$ 5–10 μm thick – the "intermediate layer"; this layer consisted for the most part of needle-shaped ettringite crystals, leaf- or flake-like $Ca(OH)_2$, sporadic needle-shaped calcium silicate hydrates (C–S–H) and "big" hexagonal $Ca(OH)_2$ crystals aligned steeply with respect to the aggregate surface;
c. the "transition zone", $\approx$ 10 μm thick which is characterized by dense paste which merged into the bulk cement paste.

Zimbelmann attributed the origin of the interfacial zone to the formation of thin films of water $\approx$ 10 μm thick on cement grains and around large aggregate particles in fresh concrete. The formation of water films on the aggregate particles seems quite likely. However, the formation of such films on the cement grains appears doubtful since mixing, placement and subsequent compaction of the concrete are likely to destroy such films. A similar explanation has been suggested by Conjeaud et al. [15], but no direct evidence of water films has been reported.

The microstructural features of the interfacial zone, which has been outlined by the foregoing investigators, have also been observed by several other workers [16–21]. The general observation is that the micro-characteristics of the paste-aggregate interfacial region in cement-based composite materials is different from that of the bulk cement matrix. Compared to the matrix, there is a high proportion of larger and better-crystallized hydrates, predominantly calcium hydroxide and ettringite. The calcium hydroxide crystals have a preferential orientation in such a way that their basal cleavage planes are nearly perpendicular to the aggregate surface. The porosity of this region is higher than the bulk matrix. A schematic illustration of the transition zone in concrete has been shown in Fig. 1.1.

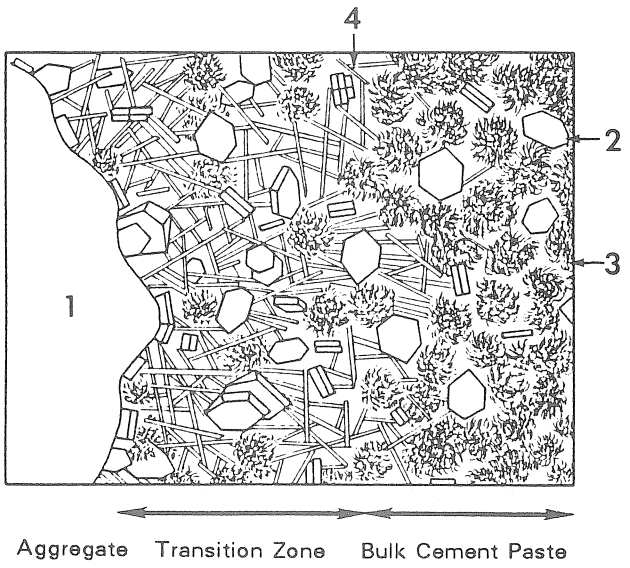

Fig. 1.1. Schematic representation of the transition zone between cement paste and aggregate in normal concrete containing no mineral admixtures. 1 = aggregate; 2 = $Ca(OH)_2$; 3 = C–S–H; 4 = Ettringite [25].

1.4 *Texture of Cement Hydration Products at the Interfacial Zone*

A recent advance in the understanding of the microstructure of the interfacial zone is concerned with the texture of the cement hydrates at the paste-aggregate interface. The texture refers to the mode of occurrence or pattern of orientation of the hydration products at the interfacial zone with respect to the aggregate surface.

A unique technique developed by Grandet and Ollivier [9, 23], based on X-ray diffraction analysis, is the most commonly known and extensively used method for studying the texture of the hydrates at the interfacial zone. This method has been exploited in the present work; details of the procedure are given in Chapters 3–5 of this paper.

Using this technique, Grandet and Ollivier presented data to indicate that calcium hydroxide crystals in the transition zone are preferentially oriented with their *c*-axes perpendicular to the aggregate surface. They found a parameter which shows the relationship between the diffraction intensities of the {001} plane and the {101} plane of $Ca(OH)_2$ crystals in the transition zone. This parameter, known as the orientation index, I_{CH} or degree of orientation, was highest (> 1.0) at the aggregate interface, and approached a value of unity in the cement matrix. Fig. 1.2 shows the orientation index, I_{CH}, versus distance from the aggregate surface for quartz and marble. The method has been used to study several factors which affect the orientation of calcium hydroxide crystals and other hydrates such as ettringite at the cement paste-aggregate interfacial zone [12].

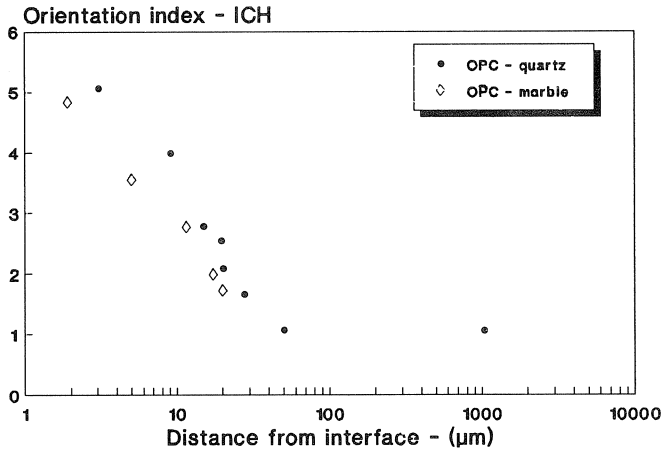

Fig. 1.2. Index of orientation, I_{CH} versus distance from polished aggregate surface for quartz and marble (Redrawn from [27]).

More recently, Monteiro and Mehta [23] used this method to study the concentration of ettringite at the interfacial zone. They demonstrated that the concentration of ettringite (expressed in terms of the X-ray diffraction intensity in counts per second) is high at the aggregate interface and decreased to a constant value in the bulk cement paste as shown in Fig. 1.3.

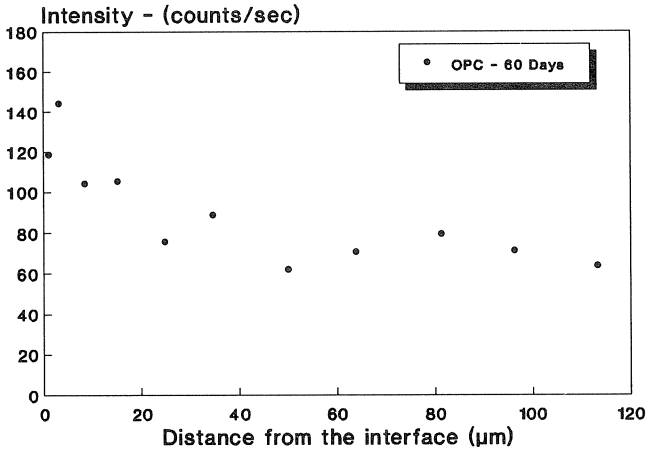

Fig. 1.3. Variation in peak intensity of ettringite as a measure of its concentration at the cement paste-aggregate interfacial zone (Redrawn from [27]).

Yuan and Guo [24] studied the structure of the interfacial zone using a combination of the technique of Grandet and Ollivier [9, 22] and bond strength measurements on cement paste-marble composites. After scanning electron microscopic observations of the debonded cement pastes-marble surfaces, they characterized the interfacial zone

(from the aggregate surface into the bulk paste) as follows. First, a duplex film consisting of very fine calcium hydroxide crystals, followed by a C–S–H film, and a porous network of ettringite and C–S–H. This description seems to be in agreement with the description given by Barnes [7, 8] and Monteiro (in Mehta [25], see also Fig. 1.3). They attributed the formation of the "duplex film" at the aggregate surface to a heterogeneous nucleation and subsequent growth of $Ca(OH)_2$ and C–S–H from an oversaturated solution. Their analysis of surface and interfacial free energies indicated that $Ca(OH)_2$ was more likely to nucleate and grow on an aggregate surface than in the bulk paste. In other words, their results showed that favourable thermodynamic conditions exist at the aggregate surface more than in the bulk paste for crystallization and growth of $Ca(OH)_2$.

The work of Yuan and Guo [24] was supported by the previous work of Yuan and Odler [26] on C_3S-marble composites, in which the overall Ca/Si moler ratio was highest at the interface and decreased into the bulk matrix. This Ca/Si trend delineated an interfacial zone of $\approx$ 100 μm thick in which the ratio was higher than 3 as shown in Fig. 1.4. These results were considered to indicate a possible migration of Ca_{2+} and OH^- ions from the bulk paste towards the interface for crystallization.

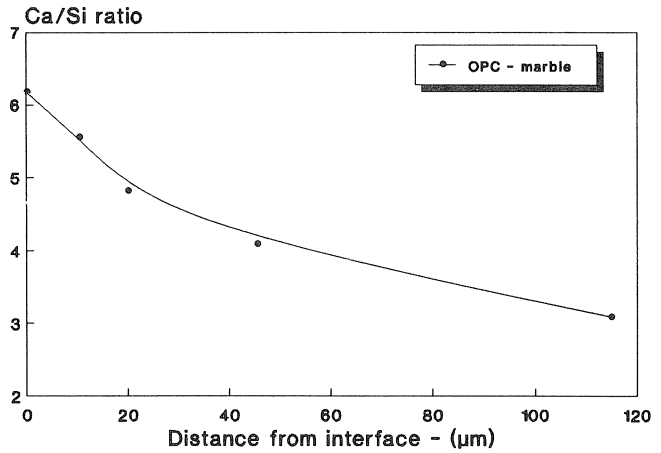

Fig. 1.4. Average Ca/Si molar ratio of the hydrated C_3S paste as a function of the distance from the marble-paste interface (Redrawn from [27]).

1.5 *Chemical Nature of the Cement Paste-Aggregate Interfacial Bond*

A number of investigations have shown that chemical reactions sometimes do occur between tricalcium aluminate (C_3A or $3CaO \cdot Al_2O_3$) which is present in portland cement and calcite from calcareous aggregates to form "carboaluminates" [27]. The assessments of the effects of these chemical reactions on strength though, have not been consistent. Cussino and Pintor [28] and Cussino et al. [29] reported that a kind

of chemical reaction occurs between calcite, C_3A or C_4AF, and water to produce $3CaO \cdot Al_2O_3 \cdot CO_2 \cdot 11H_2O$. They referred to this compound as "carboaluminate" hydrate. By examining polished marble samples covered with portland cement paste with an X-ray diffractometer, Grandet and Ollivier [22] also identified "carboaluminate" hydrates $3CaO \cdot Al_2O_3 \cdot CO_2 \cdot 11H_2O$ at the interfacial zone. Zimbelmann [30] concluded from bond strength studies that a kind of chemical reaction occurred between cement paste and limestone aggregates. This reaction, according to him, increased the bond strength. Monteiro and Mehta [31] used SEM to identify a calcium carbonate-calcium hydroxide compound, reported its XRD pattern, and suggested that the reaction was responsible for the increased strength of concrete containing limestone aggregate.

Carboaluminate hydrates have also been suggested to form between cement paste and calcareous aggregates by Yuan and Guo [24] and Yuan and Odler [26]. Using a SEM, Yuan and Guo [23] observed the surfaces of marble to be "corroded" after debonding cement paste-marble composites, like Farran [2]. According to them this "corrosion" was an indication of "dissolution" of the marble in the alkaline fluid to form $Ca(OH)_2$. The formation of the "carboaluminate" layer at the rock-cement paste interface was found to be beneficial for the marble-cement paste bond. They concluded, however, that excessive dissolution of the carbonate rock with subsequent precipitation of calcium hydroxide at the interface adversely affected the bond strength.

In the case of siliceous aggregates, chemical reaction has not yet been recognized at normal temperatures by most investigators. Zimbelmann [30] concluded from microscopic studies of the cement paste-quartz aggregate bond at a temperature of $\approx 20\,°C$ that no chemical reaction was involved. Massazza and Costa [27] reported that at relatively high temperatures of $\approx 60\,°C$, hydrolysis of lime with siliceous aggregates usually takes place to form calcium silicate hydrates. Based on bond strength data, Scholer [32] suggested later that some siliceous aggregates could produce some form of "chemical bonding", although the nature of the chemical bonding was not clearly described. No such chemical reaction involving siliceous aggregates at normal temperatures has been confirmed yet.

It appears from the foregoing section that a kind of chemical reaction involving some constituents of the cement paste and calcareous aggregates takes place at normal temperatures. The nature of the reaction and its effects on the mechanical behaviour and the durability of concrete are not well understood. Additional investigations have been carried out to clarify this issue and will be reported in this paper.

1.6 *Porosity and Grain Arrangement at the Interfacial Zone*

Considering the open microstructure of the interfacial zone, and the relatively coarser and better-crystallized hydrates, one will expect the porosity of the interface to be higher than that of the bulk cement paste. However, opinions vary on this subject. Tognon and Cangiano [33] compared the porosity of the pastes in mortars to the

porosity of neat cement pastes of the same water-cement ratios and ages, after statistically normalizing the data. Their study was done with the aid of a mercury intrusion porosimeter. They observed differences between the calculated and the measured porosimetric values and attributed the differences to the higher porosity of the interfacial zone. Kayyali [34] performed a similar study on pastes, mortars and concrete but concluded that the interfacial zone was lower in porosity.

More recently, Scrivener [17–20] has developed a method for quantitatively characterizing the paste-aggregate interfacial zone in cement composites. She used a combination of backscattered electron imaging and quantitative image analysis to study particulates at the interfacial zones in plain concretes and concretes containing mineral additives. The information obtained by this method has been shown to correlate well with quantitative information obtained by other methods such as X-ray diffractometry, mercury intrusion porosimetry, etc. [17–20]. Fig. 1.5 is a summary of the results of some of her studies. The figure shows that the amount of anhydrous cement grains is lowest in the vicinity of the aggregate, and increases into the bulk paste. Her results confirmed the observations made by Zimbelmann [14, 30], and a previous investigation by Scrivener and Gartner [19] who found little or no anhydrous cement grains within a zone of $\approx$ 15–25 μm around coarse aggregate particles. The figure also shows that the porosity, on the other hand, is highest at the interface, and decreases with increasing distance into the bulk paste. These porosity data also support an earlier study by Farran [2], who used light microscopy to examine thin sections of mortars and observed the presence in some cases of interfacial zones with increased porosity.

The higher porosity at the aggregate interface and the low amount of unreacted cement grains in the interfacial zone, have been attributed to the poor packing of cement grains,

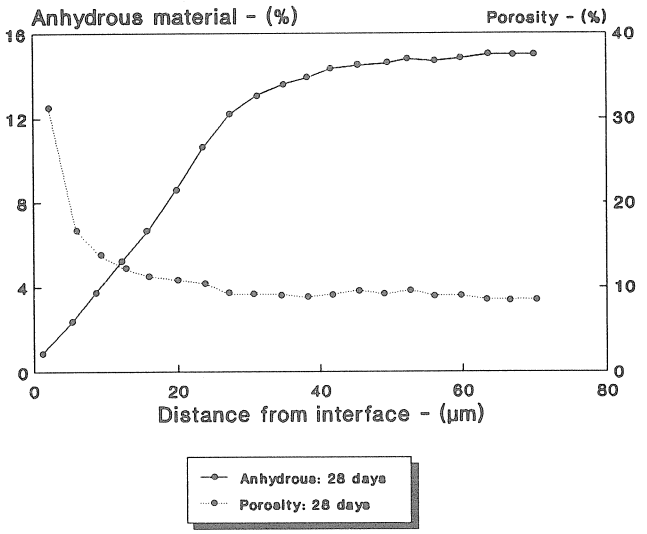

Fig. 1.5. Microstructural gradients (anhydrous material and porosity) in the interfacial region of concrete made with ordinary portland cement (Redrawn from [20]).

and to the "wall-effect" and micro-bleeding under coarse aggregate particles as illustrated in Fig. 1.6 [25].

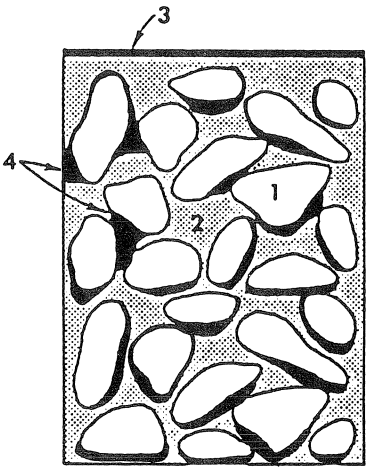

Fig. 1.6. Schematic representation of bleeding in freshly deposited concrete. 1 = Aggregate particles; 2 = Cement paste; 3 = Visible bleed water; 4 = Internal bleed water or micro-bleeding [25].

1.7 *Thickness of the Cement Paste-Aggregate Interfacial Zone*

The thickness of the cement paste-aggregate interfacial layers is usually taken to be the distance from the surface of the aggregate where the cement paste has a distinctive microstructure. It is variable depending on the type of aggregate and cement used, the water-binder ratio of the mix, the age of the composite, the nature of bonding between the paste and aggregate particles, and the method used to estimate it.

The usual thickness ranges between 50 and 100 μm. In some cement composites, however, it is found to be as thin as 1 μm [35], resembling the duplex film reported by Barnes et al. [7, 8, 13], or it could extend several microns from the aggregate surface [35]. Farran et al. [16] studied double replicas of abraded surfaces of mortars up to about 35 μm away from the aggregate surface. They found within this region, a distinct microstructure of the cement paste which was taken to represent the interfacial zone. Zimbelmann [30] reported the thickness from bond strength studies to be ≈ 25 μm, while Grandet and Ollivier [9], using a semi-quantitative X-ray technique, found this zone to be ≈ 40 μm thick. Using a SEM with secondary electron imaging to examine fracture surfaces and with backscattered electron imaging to examine polished specimens, Struble [21], and Scrivener and Pratt [18], in separate studies found the thickness to be ≈ 50 μm. In a similar study, Yuan and Odler [26] reported the thickness to be ≈ 100 μm. Their result was obtained from an estimation of the Ca/Si ratio from C_3S-marble composites using electron probe micro-analysis (EPMA).

In typical concrete systems, the thickness of the cement pastes which are "sandwiched"

between the aggregate particles ranges between 80 to 150 μm [1, 13]. Of this, the thickness of the interfacial zone ranges between 25 to 100 μm [9, 21, 27]; the volume of which represents approximately 30 to 50% of the total volume of the cement matrix. It is clear that the interfacial region forms a significant proportion of the cement paste. This emphasizes the need for a better understanding of its character and the role it plays in the mechanical behaviour and the durability of concrete.

1.8 *Microhardness of the Paste-Aggregate Interfacial Zone*

The microhardness value H_v is a useful parameter which indicates the compactness of the cement paste system. A description of this method has been given in Section 2.2.5. A lower value implies that the cement paste is either soft or contains a higher amount of micropores, which is an indication of higher porosity.

The first reported work about the microhardness of the interfacial layer was by Lyubimova and Pinus [36]. They measured microhardness across the cement paste-aggregate interface for different rocks and cements. Their results showed a variation of microhardness from the aggregate interface into the bulk paste. At a distance of $\approx$ "2-3" μm from the aggregate surface, a high microhardness value $H_v \approx 20$ was measured. This was followed by a softer region with $H_v \approx 5$, and then another zone $\approx$ 10-50 μm thick into the bulk paste - a region with a relatively constant microhardness value of about 10. The shape of the H_v distribution of the interfacial zone showed a "valley" or a "trough" representing the softer interfacial layer.

Yuji [37] obtained similar microhardness distribution using ordinary sand particles and slag particles as aggregates. From his plot, he obtained a "valley" at a distance of about 20-30 μm from the aggregate surface. The results of his study for specimens containing the sand particles are shown in Fig. 1.7.

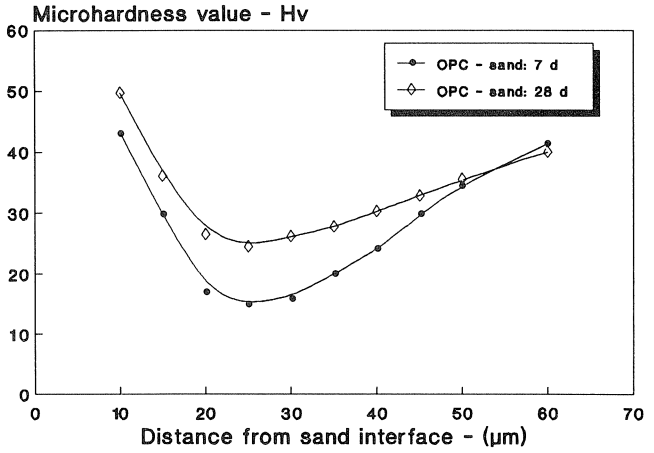

Fig. 1.7. Curves showing the distribution of microhardness values at the paste-sand interface in mortars prepared with ordinary portland cement; a = 7 days; b = 28 days (Redrawn from [37]).

The "trough"- or "valley"-shaped distribution of the H_v data in the immediate vicinity of the aggregate is an indication of the occurrence of a higher microporosity in the interface. Mehta and Monteiro also [38] investigated the effect of age on the microhardness value of the interfacial film. They observed an increase in value of about 25% from 30-day old film to 1-year old film. This suggests that as hydration progressed, the interfacial zone became gradually filled with cement hydrates.

1.9 *Strength of the Cement Paste-Aggregate Interfacial Bond*

Extensive studies on bonding in concrete by Hsu and Slate [39], Sha and Slate [40], Hsu et al. [41], Slate and Olsefki [42], and Alexander et al. [43] indicate that the interfacial bond between coarse aggregate and cement paste or mortar is the "weakest link" in concrete with respect to strength.

According to Mehta [25], the strength between the hydration products and the aggregate particles is due to the van der Waals force of attraction. Since the adhesive strength at any point depends on the volume and size of voids present, it is not surprising that the paste-aggregate interfacial zone is the weakest link in concrete. He explains that where there is crystallization of new products in the voids of the interfacial zone by slow chemical reactions between the components of the cement paste, or between some of the constituents of the cement paste and the aggregate, the adhesive strength between the paste and the aggregate could increase. Such strength contributions occur for example, when siliceous constituents of the paste, such as fly ash, silica fume and slag react with calcium hydroxide to form calcium silicate hydrates (C–S–H); or the formation of "carboaluminate" hydrates in the case of a reaction between calcareous aggregates and C_3A in the cement [22, 27–29]. On the other hand, according to Marchese [44], the large calcium hydroxide crystals in the interfacial zone tend to possess less adhesion capacity. This is because of their lower specific surface and correspondingly weak van der Waals forces of attraction. Also, because of their oriented structure in the transition zone, the large calcium hydroxide plates serve as preferred cleavage sites allowing cracks to occur preferentially along their weakly bonded basal cleavage planes.

Hsu and Slate [39] reported that with increasing age, the paste-aggregate bond strength increased. They explained, however, that the weaker bond strength compared to the tensile strength of the paste was in part, due to the formation of "bond cracks" at the aggregate interface even before the application of any load. Their work also showed the existence of "bond cracks" at the aggregate interface, even when the concrete was kept in a continuously wet environment.

1.10 *Effects of the Paste-Aggregate Interfacial Bond on the Strength of Concrete*

There are varied opinions about the effects of the paste-aggregate bond on the strength of concrete. From bond strength measurements, Alexander et al. [43] found a linear correlation between concrete strength, and the paste and bond strengths. Their results

showed that as the bond strength increased, the compressive strength of concrete also increased. On the other hand, Fagerlund [45], Hsu et al. [41], and Perry and Gillot [46], concluded that the cement paste-aggregate bond was not important to concrete strength. In fact, Perry and Gillot [46] found little effect of bond strength on compressive strength above the stress level at which bond cracks are initiated.

When concrete is subjected to load, cracks may initiate and propagate owing to the high tensile stress concentrations in the specimen (produced by interactions between the aggregates and voids within the concrete) [47]. In a detailed study about the internal behaviour of concrete subjected to stress, Hsu et al. [41] and Sha and Slate [40] observed micro-cracks in both the cement paste and at the paste-aggregate interfacial zone. The crack density at the paste-aggregate interface was found to be higher than that in the paste. Using microscopic and X-ray diffraction techniques, Hsu et al. [41] observed directly the cracking of plain concrete in compression. They reported that even before loading began, cracks were observable at the paste-aggregate interface; these "micro"-cracks or presumably "shrinkage" cracks are produced as result of the hydration of the cement. Their study showed that up to about 0.30 of the ultimate strength, f'_c, there was very little or no extension of these cracks. Beyond $0.30f'_c$, the cracks began to grow under increasing load. After about $0.50f'_c$ the "bond cracks" also began to extend through the matrix, forming bridges between the coarse aggregate particles. Finally, beyond $0.75f'_c$, the "matrix or mortar cracks" began to connect each other, forming a more extensive network. This indicates further that the cement paste-aggregate interfacial zone is the weakest region of concrete. In general, three types of micro-cracks can be distinguished [40,48]. These include:

1. *bond or adhesion cracks:* these are micro-cracks which exist at the interface between coarse aggregate and the mortar.
2. *mortar or paste cracks:* which are micro-cracks existing within the mortar or the paste, and along the interface of sand grains.
3. *aggregate cracks:* these are micro-cracks mostly in coarse, but sometimes also in fine aggregate particles.

Fig. 1.8 is a schematic illustration of these microcracks. The study of Sha and Slate [40] about failure pattern in concrete also revealed that most of the bond failures occurred within the interfacial layer.

Failures occurring directly at the paste-aggregate interface were also common. Glucklich [49] found the number of microcracks in the interfacial region to increase with increasing application of load. Studies show that by increasing the paste-aggregate bond strength the compressive strength of concrete tends to increase [50–56]. Hsu et al. [41] and Perry and Gillot [46] noticed that, by increasing the bond strength, the stress level at which extensive microcracking began also increased. This effect is the reason for the increase in brittleness with increasing compressive strength.

In a similar study, Mindess and Diamond [57, 58] reported that cracking in mortars and concretes tended to initiate at the interfacial region, and that the crack path generally ran within the interfacial zone, at a distance of a few microns from the surfaces of the aggregate particles themselves.

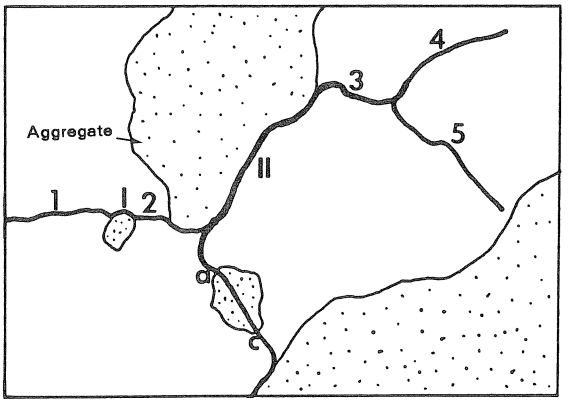

Fig. 1.8. Area containing five paste or mortar cracks marked (1, 2, 3, 4, and 5), 2 adhesion or bond cracks (marked I and II) and 1 aggregate crack (marked a-c); (Redrawn from [48]).

Thus it appears, there is a general agreement that the interfacial zone is a "weak link" in the structure of normal concrete with regard to strength. In very high strength cement paste systems, where the paste-aggregate bond is relatively strong, differences in opinion do exist as to the nature of the crack growth and propagation in mortars and concrete. While Bentur and Mindess [59] observed cracks to go around aggregate particles, Regourd [50], Sarkar and Aitcin [55], and Odler and Zurz [60] observed cracks to go through the interfacial layer at a few microns away from the paste-aggregate interface.

1.11 *Effects of the Paste-Aggregate Interfacial Zone on the Durability of Concrete*

There is little published information on direct studies relating the effects of the paste-aggregate interfacial zone on the durability of concrete. Most of the published work involve investigations in which porosity or permeability were examined. Mindess et al. [in Reference 53] and Wakely and Roy [61] and Malek and Roy [62] reported that the paste-aggregate interfacial zone does not seem to play any major role in determining the permeability of concrete, and hence may probably not influence the durability of concrete. Valenta [63, 64] and Tognon and Cangiano [33], however, reported some contrary findings. They examined the effect of the interfacial zone on the permeability and the durability of concrete from freeze-thaw and pore structural studies respectively. They showed that the interfacial layer contributed significantly to the permeability and the durability of concrete. Xie and Tang [65] performed electrical conductivity measurements on mortar specimens containing ordinary portland cement paste and quartz aggregates with the intent of delineating the effect of the paste-aggregate interfacial zone on the conductivity of mortars. Their results demonstrated that the interface material was more electrically conductive than the paste matrix. Norton and Pletta [66] presented data to indicate that increasing the volume concentration of aggregate

increased the permeability of concrete. Their results were supported by the work of Nyame [67], who studied the permeability of normal and lightweight mortars, and concluded that by increasing the aggregate volume, interfacial effects seemed to increase the permeability. Toy [68], Murata [69], and Bracs et al. [70] also demonstrated that a reduction of the maximum aggregate size reduced the permeability of portland cement-based composites. The foregoing review shows that the interfacial zone in one way or another may influence the permeability of concrete and for that matter, the durability of concrete. However, because all these studies do not directly relate the interfacial zone to the durability of concrete, one cannot tell how significant its influence may be. Further research into this effect is required to provide solutions to this problem, which is carried by the author and reported in a later chapter.

1.12 *Effects of Additives of the Portland Cement Paste-Aggregate Interfacial Zone*

1.12.1 Mineral Additives

Bentur et al. [51, 56] investigated the effects of addition of silica fume on the paste-aggregate interfacial zone. They found out that the silica fume addition improved significantly the structure of the transition zone by densifying it. Goldman and Bentur [56] observed that for the same water-binder ratio, the compressive strengths of silica fume concretes were significantly higher than those of silica fume pastes as well as those of plain (silica fume-free) concretes of the same ages. They concluded that the main beneficial effect of addition of silica fume to concretes was the result of the improvement of the structure of the interfacial zone.
Regourd [50], Sarkar and Aitcin [55], Detwiler and Mehta [71], Cheng-yi and Feldman [72], Odler and Zurz [60] and Sarkar et al. [73] all found the paste-aggregate interfacial zone to be denser in silica fume concretes than in plain portland cement concretes. In general, they found the paste-aggregate bond to be improved by addition of silica fume. In contrast to these observations, Darwin et al. [74] found lower bond strengths for mixes containing silica fume. They attributed the lower bond strength to the absence of calcium hydroxide at the paste-aggregate interfacial zone in the presence of silica fume. They also ascribed the increase in strength of the silica fume concrete to an increase in strength of the cement paste matrix rather than the interfacial zone.

Detwiler et al. [75], using the technique of Grandet and Ollivier [9, 22], investigated the influence of blastfurnace slag cement on the structure of the transition zone. They concluded that in the presence of sufficient quantity of slag (up to $\approx 30\%$ by mass of cement), less crystals were formed at the paste-aggregate interface. They attributed this to the ability of the slag to form a dense paste at the interfacial zone, thus inhibiting the transport of Ca^{2+} ions to the aggregate surface for precipitation. In a recent study Mehta and Monteiro [38] showed the amount and the orientation index of $Ca(OH)_2$ at the interfacial zone to be decreased by addition of silica fume and fly ash. They also found the thickness of the transition zone to be reduced. Saito and Kawamura [76] and Gjorv

et al. [77] have also found the thickness of the interfacial zone to be reduced by addition of pozzolans to concrete.

1.12.2 Chemical Additives

Zimbelmann [30] showed that by coating the surface of polished aggregate particles with tensides, the structure of the interfacial zone and bonding of paste to aggregate particles could be improved. Xueqan et al. [78, 79] performed similar tests using sand and limestone aggregate particles coated with water glass (sodium silicate). They found the bond strength of paste to the aggregates and the compressive strengths of mortars prepared with the pretreated aggregates to be higher than mixes containing untreated aggregates. Although the results of these studies are quite interesting, the practical potential of these techniques may be limited. This is because, on singular aggregate particles, the adhesion of the fresh paste to the treated rock surface is carefully done. So that when the cement paste is being cast against the rock, the chemical agent on the surface of the aggregate is practically not disturbed. In practice, the tumbling and shearing caused by the coarse aggregates particles in the wet mix may remove the tensides or chemical coatings which may probably reduce their effective performance.

1.12.3 Polymer Dispersions

Su and Bijen [80, 81] showed that by using acrylic polymer dispersions in conjunction with portland cement, the structure of the paste-aggregate interfacial zone could be improved. The investigation showed the adhesive strength of pastes to aggregates could be improved by using polymer-modified cement pastes. They found the amount of pore space to be decreased, and the density of cracks at the interfacial zone to be reduced.

1.13 *Concluding Remarks*

The purpose of this brief literature survey has been to highlight the microstructure of the paste-aggregate interfacial zone and some of its influence on the strength and the durability of concrete. The survey shows that in concrete, interfacial zones with distinct microstructural features exist between cement paste and aggregate particles. In general, these interfacial zones contain more calcium hydroxide than the bulk cement paste matrix. Moreover, the calcium hydroxide crystals are not randomly oriented. They exhibit a preferred orientation with regard to the surface of the aggregate.

The review also shows that most of the studies regarding the character of the transition zone have been approached from micro-level techniques, such as optical microscopy. For example, micro-porosity, micro-cracks, and cement hydration products at the interfacial zone have been observed using a scanning electron microscope. The elemental and chemical composition of the hydration products at the transition zone have been estimated by energy dispersive spectrometry (EDS/EDAX) and semi-

quantitative electron probe micro-analysis (EPMA). While nearly all investigators agree on the existence of a relatively higher amount of calcium hydroxide at the interfacial zone, differences in opinion exist on the question of porosity. One group of investigators believe that the interface is higher in porosity than the bulk paste. Others are of contrary opinion. Also, whereas there is substantial evidence that chemical reactions exist between cement paste and carbonate rocks, opinions concerning the role of these reactions on the mechanical properties of concrete are varied. Additional information is required to resolve this issue.
With regard to the role of the interfacial zone on the mechanical properties and the durability of concrete, there are also two diversified schools of thought. This aspect of the interfacial zone needs further investigation.
The survey shows that from the few attempts made to improve the structure of the interfacial zone, mineral additives, such as silica fume, pulverised fuel ash and blast furnace slag, and chemical additives such as water glass and tensides, as well as polymer dispersions seem to show considerable improvements of the microstructure of the interfacial zone.

It is important to point out from this literature study that, whereas a great deal of effort has been made to characterize the microstructure of the interfacial zone, relatively little attempts have been made to improve this weak region of concrete. This is because in the first place, the volume of cement paste constituting the interfacial zone is usually assumed to form an insignificant part of the total volume of concrete and therefore not important as far as improvements in the property of concrete is concerned. And in the second place, most of the information obtained about the character of the interfacial zone from micro-level techniques have not been adequately translated to the bulk properties of concrete such as the compressive strength and the permeability. This is perhaps the reason why at the moment there is no simple way of predicting how much improvement can be made in the overall performance of concrete through improvement of the interfacial zone.
In the following chapters the above considerations have been discussed in the light of the experimental results obtained.

2 Materials and Experimental Methods

2.1 *Materials*

In this section, a summary of the materials used for these investigations is given. In addition some characteristics of these materials and in some cases their composition are also presented.

2.1.1 Cements

The cements used for these studies included an ordinary portland cement (OPC) equivalent to ASTM Type I portland cement and a portland blast furnace slag cement (with

approximately 65–70% by mass of slag). All the cement used conformed to the Dutch Cement Standard NEN 3550. The chemical composition and other properties of these cements are presented in Table 2.1.

Table 2.1 Chemical composition of the cements

Composition (%)	Portland cement ASTM Type 1	Blast furnace slag cement (with ≈65–70% by mass of slag)
SiO_2	19.9	29.2
Al_2O_3	5.6	7.5
Fe_2O_3	2.9	1.7
MgO	1.5	6.9
CaO	62.0	49.0
Na_2O	0.2	0.2
K_2O	0.8	0.6
SO_3	3.1	2.9
Free water	0.4	0.3
Loss on ignition	0.6	0.3
Insoluble residue	4.1	3.7
Specific gravity	3,10	2,95
Specific surface (Blaine: m^2/kg)	300 ± 20	400 ± 50

2.1.2 Aggregates

The aggregates used were rock prisms of granite and limestone, a commercially available sand, a chemical grade inert (α-quartz) sand and a polypropylene plastic plate used as a "model coarse aggregate". The maximum grain size of all the sand fractions used was about 5.0 mm.

2.1.3 Mineral Additives

The mineral additives used in these investigations included three low-calcium fly ashes (FA, EFA and LM), equivalent to ASTM Class F fly ashes. The ashes FA and LM were from a dry-bottom boiler, while EFA was from a wet-bottom boiler. The chemical composition and other properties of these ashes are given in Table 2.2. Their glass contents which were determined by a quantitative X-ray diffraction technique are given in Table 2.3.

EFA has the greatest glass content. There is, however, not much difference in their SiO_2 contents. The particle size distribution of the ashes was determined with the aid of the Malvern 2600 Particle Size Analyzer. The results showed EFA to be relatively the finest of the three ashes, followed by FA and LM respectively.

The other mineral additives used were silica fume (SF), a metakaolinite (MK), and ground granulated blastfurnace slag as part of portland blastfurnace slag cement (this cement contained 65–70% by mass of slag as partial portland clinker replacement). The

silica fume and the metakaolinite existed in a powdered form and were added to the mix in the dry form. The chemical composition and other physical properties of these mineral additives are given in Table 2.4.

Table 2.2 Composition and properties of fly ashes used

Composition (%)	FA	EFA	LM
SiO_2	54.6	50.0	51.7
Al_2O	27.0	25.6	33.0
Fe_2O_3	7.6	6.5	4.8
CaO	2.9	4.3	2.0
MgO	2.3	2.4	0.5
Na_2O	0.6	2.2	0.4
K_2O	2.4	3.8	1.0
TiO_2	0.4	1.2	1.7
Water content	0.1	0.1	0.1
Loss on ignition	2.1	3.9	4.9
Specific gravity	-	2.3	-
% >45 μm	22.5	7.0	23.5

Table 2.3 Mineralogical composition of the fly ashes used

Minerals (%)	FA	EFA	LM
Quartz	4.5	1.8	5.1
Mullite	11.4	2.1	22.8
Magnetite	0.6	0.7	0.5
Total crystalline	16.5	4.6	28.4
Glass	83.5	95.3	71.6

Table 2.4 Chemical composition and other properties of the silica fume and the metakaolinite

	% (by mass)	
Chemical composition and other properties	metakaolinite MK	silica fume SF
SiO_2	55.5	95.0
Al_2O_3	39.7	0.1
Na_2O equivalent	1.9	0.3
Specific gravity	2.5	2.3
Specific surface (BET, m^2/g)	14.8	19.3
Mean grain size (μm)	1.4	0.1

2.1.4 Superplasticizers

The superplasticizer used throughout the study was an aqueous solution of sulphonated naphthalene formaldehyde (Conplast^R).

2.2 *Experimental Procedures*

2.2.1 Calcium Hydroxide Content Determination

The calcium hydroxide content was determined by the method of chemical extraction using Franke technique [82] and semi-quantitative X-ray diffraction analysis (XRD). To reduce surface bleeding and to improve uniform mixing during hardening, the sealed specimens were rotated on a rotating device at a relatively low speed for periods between 4 and 24 hours depending on the water-cement ratio of the mix. The following standard procedure was employed.

The samples were cast into plastic tubes, sealed and stored in a fog room at a temperature of about 20 °C. At the required age for analysis, a representative sample of the specimen was oven-dried at 105 °C to a constant weight and the free water content determined. Later, the sample was ground to a high degree of fineness and 0.5 g of the dry sample was then added to 25 ml of a mixture of acetoacetic ester and isobutyl alcohol (30 ml acetoacetic ester + 200 ml isobutyl alcohol) and stirred. The mixture was boiled for 1 hour, filtered, and the residue washed with 20 ml of isobutanol once. After washing, 20 ml of methanol was mixed with the filtrate and titrated against HCl (0.1 M), using bromophenol blue (1 ml) as an indicator. The end point occurred when the solution changed from blue to yellow.

In order to calculate the calcium hydroxide content in the samples, the free and non-evaporable water contents of the composites were required. These parameters were determined for each of the specimens using the standard procedures (BS 1881, Part 6) on representative samples. For each specimen, three analyses were made; the average value of the three data was considered as the representative value for the specimen.

2.2.2 Semi-Quantitative XRD Analysis

One of the techniques commonly used to evaluate the degree of preferred orientation of calcium hydroxide (CH) crystals at the interfacial zone and to characterize the extent of the transition region is the method developed by Grandet and Ollivier [9]. This is a two-step technique that involves casting of cement paste onto a piece of rock to form a composite specimen followed by X-ray diffraction analysis of the debonded paste surface to obtain some information about the interfacial zone. The most important parameter used is the orientation index of CH crystals within this transition region. In one of the studies a polypropylene plastic plate was used for studying the influence of cement paste and mortar on the microstructure of the transition zone. Obviously, the polypropylene plastic plate is not used in concrete as an aggregate, however, in the present study, it was used as a "model coarse aggregate".

Also, experience from the trial tests showed that after separation of the composite specimens some of the paste adhered to the limestone rock specimens which were used during the trials. This made the estimation of the distance from the aggregate surface and the overall data inaccurate. The use of the plastic plate enabled easy separation of the cement paste from the plate without any remnants on the plate. Although paste-

aggregate specimens cast in this way do not adequately simulate the real paste-aggregate composite in mortars and concretes, for reasons of comparison, the test results could provide an indication of the characteristics of the interfacial zone. In mortars and concrete, the shearing and tumbling of the solid particles during mixing tends to improve the packing of the grains. Lack of such mixing effects in the case of pastes, such as in this study, may serve as a limiting factor. However, since the same substrate is used, the data obtained from the test could provide a good indication of the effects of sand on the microstructure of the interfacial zone.
The water-cement ratio of the composites was 0.30 and the "(α-quartz)"-cement ratio of the "mortar" specimens was 0.40. After mixing, placing and compaction (by means of vibration), all the mixes were stored in a fog room at approximately 20 °C until they were required for testing. The specimens meant for the XRD studies were stored in sealed plastic jars under nitrogen to prevent carbonation. At the specified periods of curing (7 and 100 days), the specimens were removed from the fog room and stored in a desiccator. The drying process caused shrinkage of the specimens which easily separated at the plastic interface. The freshly-separated surfaces of the specimens at the paste side were then analyzed with a Philips X-ray PW1130 diffractometer using CuKα radiation generated at 40 kV, 20 mA. The goniometer in the diffractometer had 1^0 scatter slits, 0.1^0 resolving slits, and a scanning speed of 1^0 2Θ per minute.

As mentioned already, the parameter that is used to characterise the texture of the calcium hydroxide crystals at the interfacial zone is the orientation index, I_{CH}. This index is obtained by measuring the X-ray diffraction intensities of the {001} and the {101} planes of the CH crystals after successive abrasion of the transition zone to estimate its thickness. The method is based on the fact that in the bulk paste matrix the CH crystals are randomly oriented. The ratio R, between the $I\{001\}$ and $I\{101\}$ peak intensity of randomly oriented CH crystals is 0.74, and the orientation index, I_{CH} defined as:

$$I_{CH} = \frac{I\{001\}/I\{101\}}{0.74} \tag{1}$$

Values of I_{CH} higher than 1.0 imply preferential orientation of these crystals in such a manner that their c-axes are perpendicular to the aggregate interface. In other words, within the interfacial zone the parallel plates (or stacked plates) of the calcium hydroxide crystals are oriented parallel to the aggregate surface.
In order to obtain the same surface texture of the rock prisms, and to enable accurate estimation of the thickness of the interfacial zone, all the rock prisms were polished to the same surface smoothness. The pastes were then cast onto the polished surface of the rock prisms to form paste-rock composites. The X-ray analysis was done in combination with successive abrasion of the paste surface to estimate the thickness of the transition zone.
Recently some workers [19, 18] have questioned the applicability of this method as a means of simulating the situation in real concrete, suggesting that formulation of the

composite specimens whereby a relatively thick mass of cement paste is cast onto a flat and polished piece of aggregate does not adequately simulate the mixing processes that occur in real mortars and concrete. In the paste-rock composites, lack of shearing and tumbling of the aggregates during mixing, placement and compaction, which in the case of real concretes and mortars is known to improve the packing of the solids, serves as a limiting factor. In particular, in the presence of very finely-divided mineral additives such as silica fume, the mixing processes in real concrete are believed to play a major role in the dispersion of such particles. Observations of agglomerations in silica fume pastes as opposed to good dispersion in mortars and concretes have been made with regard to silica fume particles [18]. The present author shares similar views with these workers about the limitations of the Grandet and Ollivier technique. It may be assumed, however, that the mixing affects only the size of the weak interfacial zone but for purposes of comparison, the technique provides a good indication of the effects of additions on interfacial microstructure.
The orientation index and density determination of pastes (by helium pycnometry) were used to determine the extent of the interfacial zone for various paste-aggregate combinations.

2.2.3 Scanning Electron Microscope Studies

For the scanning electron microscope (SEM) studies, portions of specimens were cut and freeze-dried to prevent further hydration. After that, freshly-fractured surfaces were coated with a thin film of nickel or gold, mounted onto stubs, and examined using a JEOL, JSM-840A SEM. The SEM was equipped with an energy dispersive X-ray analyzer (EDAX).
In order to perform quantitative analyses (electron probe microanalyses, EPMA), the specimens needed to be polished to a high degree to remove almost all relief. This was achieved with the aid of a suitable polishing device consisting of a synthetic cloth impregnated with 1.0 μm diamond from an aerosol spray with alcohol. Prior to polishing, the specimens were reinforced with an epoxy resin by vacuum-impregnation. After polishing, a thin coating of carbon and nickel was evaporated onto the cleaned surface for subsequent examination and analysis in the SEM.

2.2.4 Microhardness Measurements

The measurements were made using a microhardness tester, Leitz Miniload 2. The composite specimens were cast into a cylindrical polypropylene plastic tube (a small mould) with the rectangular rock prism (granite or limestone) in the middle. The surfaces of the rock prisms were polished to remove nearly all form of relief before using for the test. Prior to testing, the specimens were sawn into two halves. The middle sections were then well-polished (till No. 1000 grit) with silicon carbide and alcohol before measuring the hardness. Using the pyramidal indenter in the microhardness

setup, indentations were made on 28-day old pastes with and without silica fume. From the impressions made, the Vickers microhardness values, H_v of the cement pastes in the vicinity of the aggregate were calculated.

2.2.5 Specimen Preparation for Durability Studies

All the mixes designed for the durability tests were prepared with a laboratory type, table-top Hobart Model A-200 mixer. The materials were proportioned by mass and mixed according to standard methods of mixing as detailed in ASTM C-109. The water-cement ratios were 0.30, 0.40 and 0.50; and the sand-cement ratios (by mass) were 0, 1.0 and 2.0. Following mixing, each specimen was cast separately into $100 \times 100 \times 100$ mm^3 steel moulds, carefully compacted by vibration, and then transferred into a fog room at approximately 20 °C. After 1 day the specimens were demoulded and cured in lime-saturated solutions at 20 °C until they were required for testing. At required ages of testing, the blocks of pastes or mortars were removed from storage and cored into cylinders or sawn into slices for testing. In a preliminary water absorption study (on 35 mm diameter and 10 mm thick slices, cut from 35 mm diameter and 100 mm long cores of pastes and mortars), the top and bottom 20 mm portions of the specimens (in the direction of casting) were found to have relatively variable water absorptivities, presumably due to particulate settlement before hardening. The middle 60 mm portion was found to have nearly constant water absorptivity [83]. For this reason, in all the tests (on specimens with water-cement ratios of 0.40 and 0.50), the top 20 mm and the bottom 20 mm portions of the blocks (in the direction of casting) were sawn off and were not used for further studies. Surface bleeding was observed and measured for the ordinary portland cement pastes and mortars with water-cement ratios of 0.50. However, an estimation of the effective water-cement ratio after hardening showed that the measured amount of bleeding had not changed the original water-cement ratio significantly. The effective water-cement ratios of both the cement pastes and the mortars were comparable, therefore no corrections were made for the compressive strength data obtained.

2.2.6 Pore Size Distribution Studies

Information on the pore size distribution of pastes and mortars was obtained with the aid of a mercury intrusion porosimeter. The size of the specimens used for this test was approximately 2.5 g. All the specimens were oven-dried at 105 °C to a constant weight before testing. A Carlo Erba Porosimeter-2000, with a maximum pressure of 200 MPa was used for the study. A contact angle of 141.3° was assumed throughout the testing. In addition to mercury intrusion posimetry, the density of all the specimens were also determined by helium pycnometry.

2.2.7 Rates of Diffusion of Cl^- and Na^+ into Specimens

The rates of diffusion of Cl^- and Na^+ ions into plain portland cement pastes and corresponding mortars were monitored using two compartment diffusion cells similar to the cells used by Kondo et al. [84]. The specimens consisted of $100 \times 100 \times 5$ mm^3 rectangular plates removed from the central portions of $100 \times 100 \times 100$ mm^3 blocks of cement pastes and mortars with the aid of a diamond saw. The water-cement ratio of the mixes was 0.40 and the sand-cement ratio of the mortars was 1.0. For each block, at least six to eight plates were removed. The end 20-mm pieces of the blocks were discarded and not used in any of the subsequent studies. After sawing, the plates were stored in $Ca(OH)_2$ saturated solutions until they were required for testing.

Prior to the diffusion test, the surfaces of each of the plates were carefully polished with a 600-grade emery paper, rinsed with de-ionized water, surface-dried with a tissue before being fitted into the diffusion cells. The edges of the plates in contact with the container were sealed with a vaseline gel. After fitting and sealing the test specimens in place, the cells were filled at one side with saturated $Ca(OH)^2$ solution at room temperature of 20 ± 2 °C and at the other side with 0.5 M NaCl in saturated $Ca(OH)_2$ solution. The volume of each compartment was ≈ 1500 ml. The experimental setup for which Cl^- and Na^+ diffusion was studied is shown in Fig. 2.1.

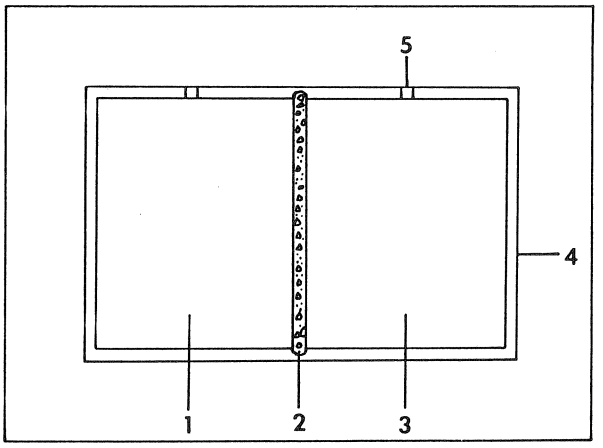

Fig. 2.1. Experimental setup for one of the diffusion cells used in the ionic diffusion study (1 = saturated $Ca(OH)_2$ solution + 0.5 N NaCl; 2 = specimen (paste or mortar); 3 = sat. $Ca(OH)_2$ solution; 4 = container (polypropylene plastic); 5 = opening for collection of samples.

After various diffusion times, the concentrations of Cl^- and Na^+ ions were determined by removing 20 ml portions of the solutions from each cell for analyses. The Cl^- concentration was determined by titration, and that of Na^+ by inductively coupled plasma spectrometry (ICP). The titration method involved addition of an appropriate excess

volume of silver nitrate, $AgNO_3$ solution and titrating against potassium thiocyanate, KCNS solution. Ammonium ferric sulphate was used as an indicator (Volhard method).
Sampling of the solutions was done after 3, 5, 7, 14, 21, 28 and 35 days. The combined volume of samples taken from each compartment was $\approx 9\%$ of the total volume of solutions in each compartment. But because at every period of sampling, equal volume of solution was removed from each cell, the errors possibly involved with this method of sampling was assumed to be negligible.

After the experimental setup was completed, there was an initial delay time during which diffusion of Cl^- and Na^+ across the 5 mm-thick specimens was established. At the onset of diffusion, the ion flux, J entering solution B is given by:

$$J = D_i \cdot \frac{(C_a - C_b)}{l} \tag{1}$$

where,

D_i = diffusion coefficient of Cl^- or Na^+
l = thickness of the specimen
C_a = concentration of ion within the specimen at the surface adjacent to solution A
C_b = concentration of ion within the specimen at the surface adjacent to solution B

However, during the test C_a and C_b could not be measured, so the ionic concentrations of solutions A and B, that is, C_A and C_B were measured.

From kinetics of ionic diffusion, the ion flux entering solution B is also given by:

$$J = \frac{V \cdot dC_B}{A \cdot dt} \tag{2}$$

where,

V = volume of solution B
A = surface area of specimen transmitting the ions

Combining Equations (1) and (2) and intergrating between the time of initial ion diffusion into solution B, that is, time, t_0 and a subsequent time, t, and assuming that C_A remained constant over the diffusion period, gives

$$\log_e \left\{1 + \frac{C_B}{(C_A - C_B)}\right\} = \frac{D_i \cdot A}{Vl}(t - t_0) \tag{3}$$

Hence, for $C_A \gg C_B$, then

$$C_B \approx \frac{D_i \cdot A}{Vl} C_A(t - t_0) \tag{4}$$

Thus, the (effective) diffusion coefficient D_i, could be calculated from slope of the rectilinear plot of C_B against t [84–88].

2.2.8 Compressive Strength Determination

The compressive strengths of the pastes and corresponding mortars were determined on $40 \times 40 \times 40$ mm^3 cubes under saturated-surface dry conditions. The mixes were formulated by mixing first the sand and the cement at a low speed. This was followed by addition of part of the water (while mixing at a moderate speed) and the superplasticizer to form a slurry. The metakaolinite or silica fume was then added and mixed at a relatively higher speed for 1 minute. The final stage lasted for a period of 2 minutes (after a pause of 1 minute) during which the rest of the water was added. The total mixing time lasted for 10 minutes. The corresponding pastes were prepared in the same manner except that the mixing time for the blends was extended to 15 minutes to break any agglomerates formed. All the specimens were stored in plastic-covered moulds in a fog room at 20 °C for 1 day, and then demoulded and cured in lime-saturated solutions until required for testing. The curing period ranged from 1 day to 3 months. For each mix, and at a specified age, three specimens were tested (uniaxial compression up to the ultimate compressive strength f_c; because the variability in the data was low, the average value of the three data was considered as the representative value.

3 Micro-Characteristics of the Interfacial Zone in Portland Cement Mortar and Concrete

3.1 *Introduction*

In this chapter, the micro-characteristics of the cement paste in mortars and concretes have been presented in relationship to the hydration of ordinary portland cement. A distinction has been made between the structure of the bulk cement paste and that of the interfacial zone on the basis of the microscopic data obtained. The possible factors that control the formation of this interfacial zone in portland cement mortars and concretes have been enumerated and discussed. Finally, some of the possible means that may be used to improve the microstructure of the interfacial zone (which have been discussed further in Chapter 5) as measures of controlling the micro-mechanical properties of the interfacial zone as well as the bulk properties of mortars and concretes have been proposed.

3.2 *Microstructure of the Cement Paste*

On a micro-scale, portland cement mortars and concretes may be considered to be composed of varying sizes of aggregate particles cemented together by a binder – the cement paste. This cement paste is assumed to be homogeneous and to consist of a solid phase that is separated by voids or pores. In the present study, the foregoing assumption about

the structure of the cement paste is investigated. The techniques that were used for these investigations have already been outlined in Chapter 2.
Figs. 3.1, 3.2 and 3.3 are SEM-micrographs of fractured surfaces of mortar specimens showing the structure of the cement paste. Directly on the aggregate surface (Fig. 3.1), there is a thin layer of cement paste ($\approx$ 1–2 μm thick, marked "D") consisting mostly of

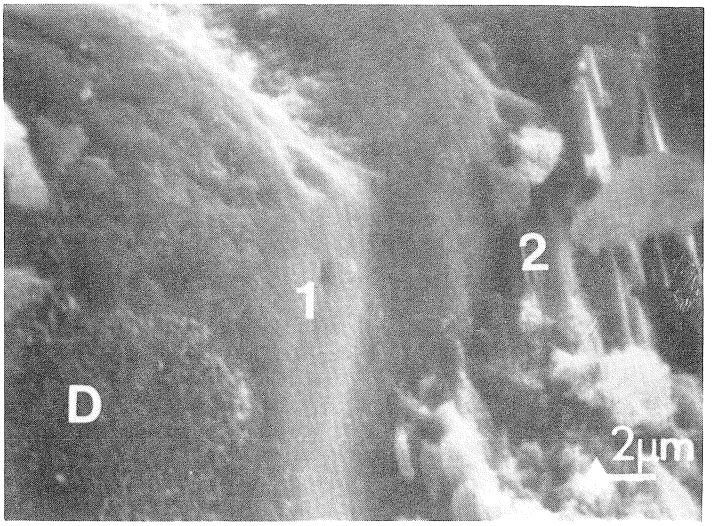

Fig. 3.1. SEM micrograph of a freshly fractured surface of 1-day old portland cement mortar showing the occurrence of the "duplex film" on the aggregate surface (w/c = 0.40); 1 = sand; 2 = calcium hydroxide crystals; D = "duplex film".

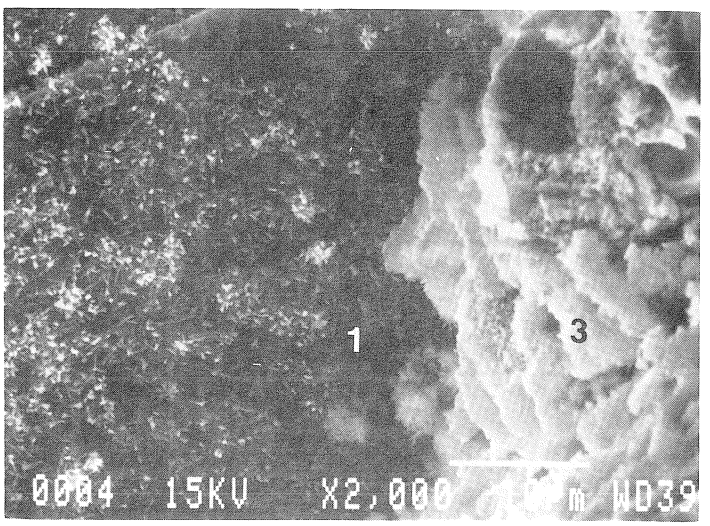

Fig. 3.2. SEM micrograph of a freshly fractured surface of 1-day old portland cement mortar showing details of the "duplex film" on the aggregate surface (w/c = 0.40); 1 = sand; 3 = cement paste.

very fine subcrystalline to amorphous material that is in intimate contact with some of the aggregate particles. Fig. 3.2 is an enlarged microphoto of a "duplex film" on one of the sand particles showing details of the duplex film at a very young age (1-day old). The structure of this layer is similar to the "duplex film" reported by Diamond [13]. This layer is followed by a relatively more crystalline phase with variable thickness ranging from (0 to more than 50 μm) containing crystalline materials such as calcium hydroxide and needle-like ettringite crystals with less amount of C–S–H. Since crystals tend to grow more easily in open spaces or voids such as in Figs. 3.4 and 3.5, the occurrence of more crystalline materials suggests that the interfacial zone is relatively more open or

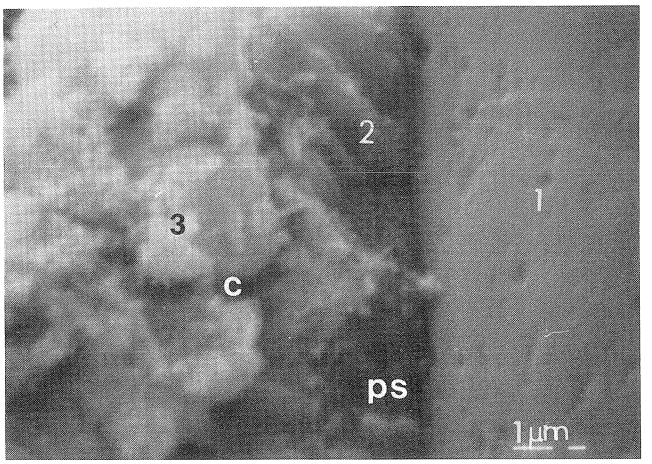

Fig. 3.3. SEM micrograph of a freshly fractured surface of 100-day old portland cement mortar showing the occurrence of the structure of the interfacial zone (w/c = 0.40); 1 = sand; 2 = calcium hydroxide crystals; c = crack of fracture; p = pore space.

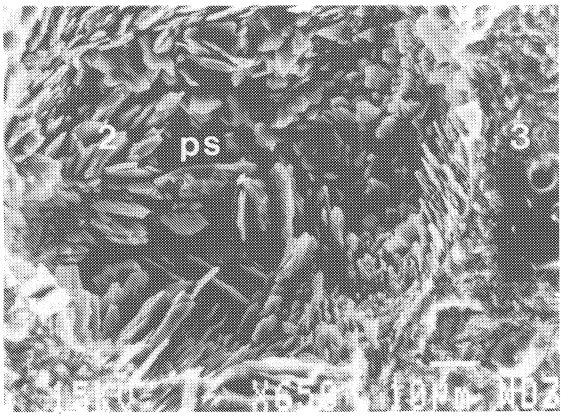

Fig. 3.4. SEM micrograph of a freshly fractured surface of 7-day old portland cement paste showing the calcium hydroxide crystals in a pore within the cement paste (w/c = 0.40); 2 = calcium hydroxide crystals.

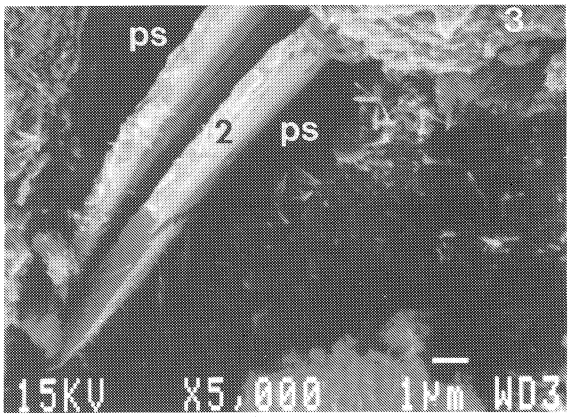

Fig. 3.5. SEM micrograph of a freshly fractured surface of 28-day old portland cement mortar showing the calcium hydroxide crystals in a pore within the cement paste (w/c = 0.40); 2 = calcium hydroxide crystals; p = pore space.

porous. Figs. 3.1, 3.2 and 3.3 also show that some of the calcium hydroxide crystals seem to have crystallized directly on the surface of the aggregate particles. The surfaces of the sand particles seem to be favourable sites for crystallization of calcium hydroxide.

3.3 *CaO and SiO_2 Distribution in the Interfacial Zone*

Fig. 3.6 shows the CaO and SiO_2 data (expressed as Ca/Si) that were obtained on polished specimens by area and spot analyses of the cement paste in the transition zone and the bulk paste. The spot analyses data were obtained at intervals of 2 to 10 µm away from the sand surfaces towards the bulk paste with a spot diameter of 0.5 µm. The

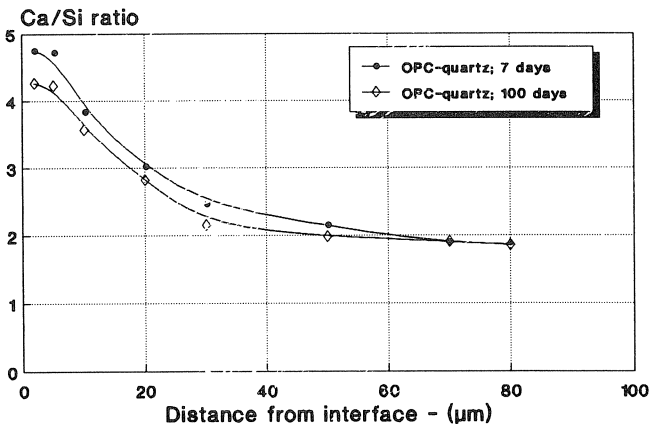

Fig. 3.6. Distribution of the Ca/Si ratio of the cement paste at the interfacial zone for 7- and 28-day old mortars (w/c = 0.40).

take-off angle was 40^0, the accelerating voltage was 15 kV, and the counting time was 50 seconds. In all about 200 spot analyses were made for the 7 and 28-day old specimens. The analyses were somehow selectively done in the sense that distinctively visible crystals of calcium hydroxide and ettringite were avoided as much as possible during the analytical processes. The results (average data at various distances from the aggregate interface) have been presented in Fig. 3.6. The data show that for both the 7 and the 28-day old specimens, the Ca/Si values tend to be higher at the aggregate interface and decreases gradually into the bulk paste. This suggests that at the interfacial zone the paste is richer in CaO than in the bulk paste. The values tend to increase with increase in age presumably due to increased hydration of the cement. For the interfacial region, the average Ca/Si values were 2.97 and 3.08 for the 7 and 28-day old specimens respectively. In the bulk paste, the values obtained for the same ages were 1.83 and 1.86.

The higher Ca/Si values of the paste in the transition zone suggests that the structure and composition of the paste in this region is different from that of the bulk cement paste. The results also suggest that the paste in the interfacial zone may be intermixed with very fine crystals of $Ca(OH)_2$ or ettringite [24, 26]. Calcium hydroxide is also known to occur as a semi-crystalline to amorphous particles within the C–S–H phase [89].

3.4 *Texture of $Ca(OH)_2$ at the Interface and Thickness of the Interfacial Zone*

The texture of calcium hydroxide at the interfacial zone and thickness of the interface were characterized by means of a semi-quantitative x-ray diffraction analysis on ordinary portland cement pastes and mortars of variable water-cement ratios and ages. The technique was also used to examine the influence of fine sand particles on the pattern of crystallization of calcium hydroxide at the paste-aggregate interface. All the techniques and principles used in this investigation have been outlined in Section 2.2.2.

Figs. 3.7 and 3.8 show the degree of orientation of calcium hydroxide crystals at the cement paste-"aggregate" interfacial zone for ordinary portland cement pastes and mortars of water-cement ratio 0.30. The data have been plotted as a function of distance from the aggregate interface. The figures also show the influence of the fine sand particles in the cement paste that is, "mortar" on the orientation index. It appears from the figures that three distinct trends can be seen:

- in the first place, the orientation index of the calcium hydroxide crystals at the aggregate interface is high and approaches a value of 1.00 in the bulk cement paste; this feature is eminent in all the neat cement pastes as well as the mortar, regardless of the age of the specimens;
- secondly, the orientation index values for the calcium hydroxide crystals at the interfacial zone is higher for the cement pastes than for the mortars for the two ages for which analyses were done; for both ages also the extent or width of the interfacial zone is shorter for the mortars than for the pastes; in the latter case, precipitation of

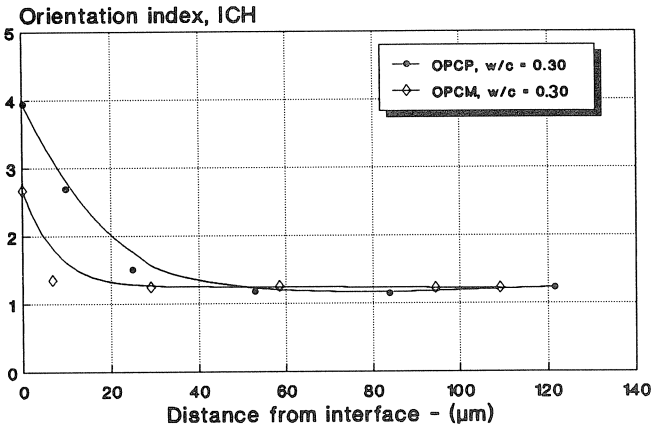

Fig. 3.7. Degree of orientation of calcium hydroxide crystals at the paste-"coarse aggregate" interfacial zone for 7-day old cement paste and mortar (w/c = 0.40).

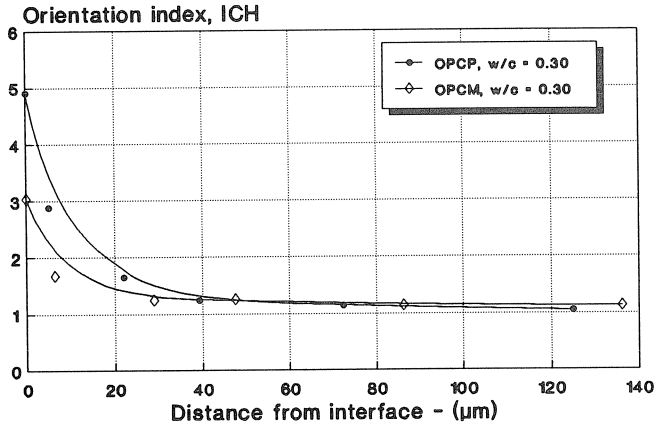

Fig. 3.8. Degree of orientation of calcium hydroxide crystals at the paste-"coarse aggregate" interfacial zone for 100-day old cement paste and mortar (w/c = 0.40).

calcium hydroxide crystals on the fine sand particles (which are nearly homogeneously distributed) within the mortar specimens is likely to be responsible for the lower values of the I_{CH} in the interfacial zone of the mortar composite; the precipitation of the $Ca(OH)_2$ on the sand particles in the mortars as shown in Figs. 3.9 and 3.10, is likely to have reduced the amount of Ca^{2+} and OH^- ions that are transported to the aggregate (larger aggregate) surface for precipitation; as a consequence, the values of I_{CH} for the mortars become lower than those for the pastes;

- finally, from Figs. 3.7 and 3.8, the orientation index values appear to be higher for the older specimens than for the younger specimens; this implies that with time, the calcium hydroxide crystals increase in size which apparently increases the degree of orientation at the interface.

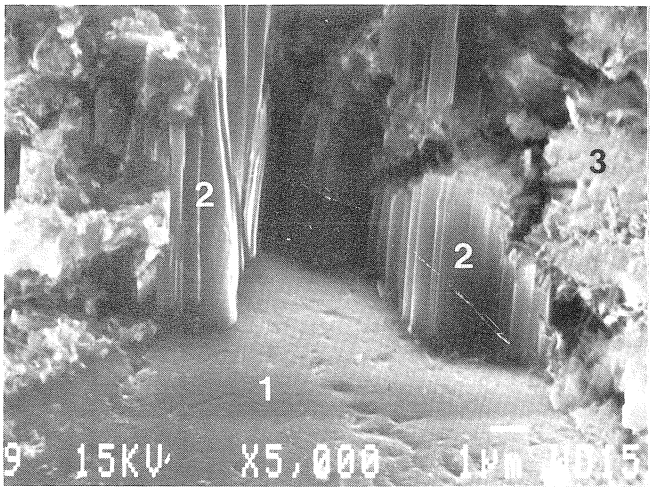

Fig. 3.9. SEM micrograph of a freshly fractured surface of 7-day old portland cement mortar showing calcium hydroxide crystals in intimate contact with the sand particle (w/c = 0.40); 1 = sand particle; 2 = calcium hydroxide crystals; 3 = cement paste.

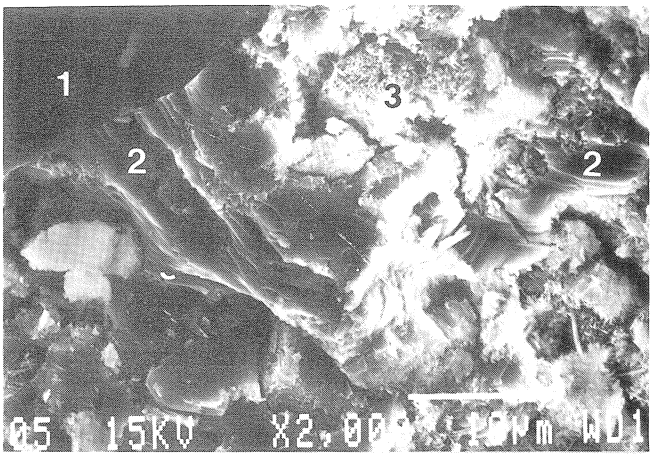

Fig. 3.10. SEM micrograph of a freshly fractured surface of 28-day old portland cement mortar showing the calcium hydroxide crystals in direct contact with the sand (w/c = 0.40); 1 = sand particle; 2 = calcium hydroxide crystals; 3 = cement paste.

Using the same technique and principles as outlined in this section, the orientation index, I_{CH}, and the thickness of the interfacial zones, δ, for various composites at specified ages were calculated. The results have been summarised in Table 3.1.

Table 3.1 Maximum orientation index of $Ca(OH)_2$ crystals I_{CHmax}, and thickness of the interfacial zone, δ for cement paste-granite composites at various ages of curing and water-cement ratios (the data in brackets were obtained using polypropylene plastic plate as a "model coarse aggregate"; n.d. = not determined; the average data of three specimens were used for each figure)

Age of the specimens	Ordinary portland cement ASTM Type I (w/c = 0.30)	Ordinary portland cement ASTM Type I (w/c = 0.40)
7 days:		
orientation index, I_{CHmax}	3.3 (5.0)	2.9
thickness, δ (μm)	53.8 (54.5)	49.4
28 days:		
orientation index, I_{CHmax}	3.6 (5.9)	n.d.
thickness, δ (μm)	32.7 (51.4)	n.d.
100 days:		
orientation index, I_{CHmax}	4.0	3.4
thickness, δ (μm)	50.3	43.0

From the data in Table 3.1, the maximum and minimum δ-values of the mixes are $\approx$ 54.5 μm and 32.7 μm respectively. Considering the thickness of the ribbons of cement paste in normal concrete to be $\approx$ 80–150 μm, with an average of about 100 μm, then using these data, a simple mathematical analysis shows that the interfacial zone occupies about 30 to 50% of the total volume of cement paste in normal concrete. This calculation is done with the assumption that such interfacial zones do occur at the interface of nearly all aggregate particles. In practice, this may not necessarily be the case. The development of the interfacial zone is very much dependent on the composition and nature of the fresh mix, among others, the initial water-cement ratio, the type of portland cement, the mixing temperature, method of mixing and whether or not chemical additives are present.

3.5 *Porosity of the Interfacial Zone*

Fig. 3.11 shows the results of the pore size distribution studies for the 100-day old samples prepared at a water-cement ratio of 0.40, and sand-cement ratios of 0, 1.0 and 2.0. In practice, there are only a few mortars that may be prepared with these compositions. In the present fundamental study, however, these compositions were chosen in order to investigate the effect of the interfacial zone on the overall porosity and pore size distribution of mortars. The data in Fig. 3.11 were calculated as percent of the total volume of mortars. Fig. 3.11 shows that as the volume proportion of the sand increases from 0 to 2.0, the capillary porosity ($r > 0.1$ μm) also increases by a calculated factor of 15. When, however, all the pores, down to $\approx$ 0.003 μm are considered,then the paste has the maximum total porosity. The total porosity appears to decrease with increasing volume of the sand in the mortar.

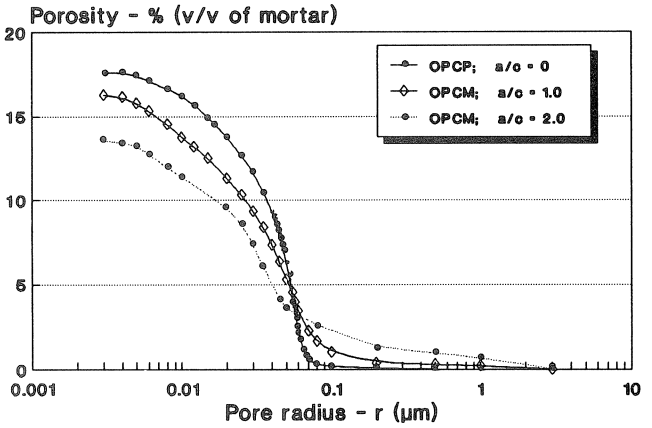

Fig. 3.11. Pore size distribution of mortars plotted as volume percent of the mortar (w/c = 0.40; age = 100 days).

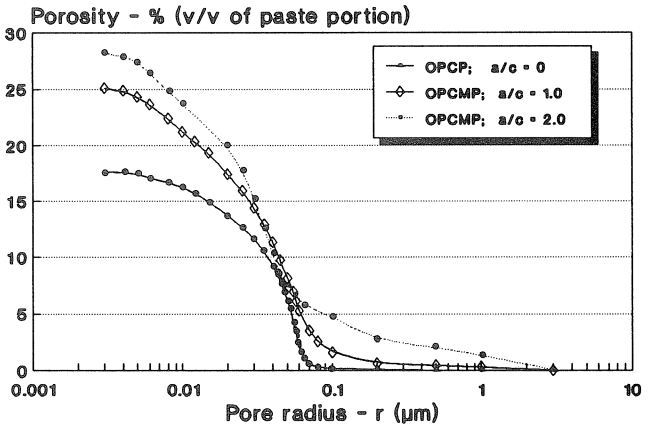

Fig. 3.12. Pore size distribution of mortars plotted as volume percent of the paste portion in the mortar (w/c = 0.40; age = 100 days).

The porosity and pore size distribution data that have been presented on the basis of the total volume of the mortar as shown in Fig. 3.11 may be limited in meaning especially, when the effect of the interfacial zone is to be examined. This is because, as the sand volume increases, the proportion of the paste in the sample (which contains the pores) decreases. Since the sand particles are non-porous, the amount of voids or pores also decreases by virtue of the decreasing volume of paste. For meaningful comparison, the porosity and pore size distribution data were calculated as percent by volume of the paste portion of each mortar. This was done in two steps.

First, the volumes of the components of the mortars, that is, cement, sand, and water, were calculated using their densities. Then the volume of sand was subtracted from the total volume of the original mix to obtain the paste volume. The paste portions were

then used to "normalize" all the data. The results are presented in Fig. 3.12. The curve labelled ***OPCMP*** represent the "normalized" data. It can be seen that as the volume of the sand in the mortars increases the total porosity of the paste in the mortars, down to ≈ 0.003 μm now increases. The plots also show a marked increase in capillary porosity – a calculated factor of about 70 as the volume proportion of the sand increases from 0 to 2. Similar effects have been observed by Feldman [89].

3.6 *Microcracks in the Interfacial Zone*

Figs. 3.13 to 3.16 show the pattern of microcracking and microfracture in the mortars. Three types of microcracks can be distinguished. These are:

1. microcracks which occur preferentially at and along the interface between the sand particles and the cement paste;
2. microcracks which occur in the cement paste; and
3. microcracks which run preferentially through the large plates or crystals of calcium hydroxide (Figs. 3.13 and 3.14) into the cement paste.

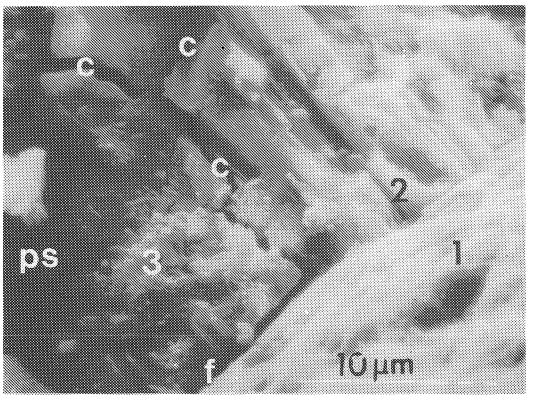

Fig. 3.13. SEM micrograph of a freshly fractured surface of a 100-day old portland cement mortar showing the character of the paste-sand interfacial zone (w/c = 0.40); 1 = sand particle; 2 = calcium hydroxide crystals; 3 = cement paste; c = crack; f = fracture.

From the micrographs most of the cracks seem to result from the shrinkage associated with the drying of the specimens prior to observation in the SEM. Investigations, however, reveal that fine, poorly-defined shrinkage cracks also do exist at the paste-sand interfaces in the wet state of the specimen prior to drying, and also before application of any load [34, 41, 57]; such fine microcracks are likely to have been caused by the shrinkage that is associated with the hydration of the cement. Not all the microcrack and fracture patterns that were observed in the mortars were observed in the plain cement paste. In the plain cement pastes only fine, tortuous microcracks were observed. Similar observations were made by Bentur and Mindess [59] and Mindess and Diamond [57, 58].

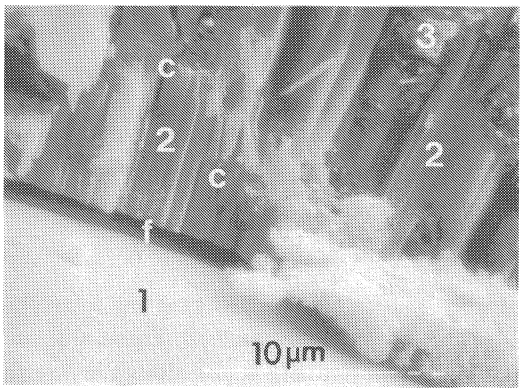

Fig. 3.14. SEM micrograph of a freshly fractured surface of 28-day old portland cement mortar showing the occurrence of calcium hydroxide at the paste-sand interfacial zone (w/c = 0.40); 1 = sand particle; 2 = calcium hydroxide crystals; 3 = cement paste; c = crack; f = fracture.

3.7 *Concluding Remarks*

The results of the investigations in this chapter show that the microstructural features of the interfacial zone between portland cement paste and the aggregate particles in concrete are considerably different from those of the bulk cement paste matrix.

The formation of the "weak interfacial" region in ordinary portland cement concrete is likely to be the result of two effects:

(i) micro-bleeding, which causes "pockets" of water to be entrapped around the aggregate particles, and

(ii) inefficient packing of the cement grains ($\approx$ 10–30 μm average diameter) at the aggregate interface, otherwise known as the "wall effect", which causes less cement particles to come close to the surface of the aggregate.

These two factors are the result of the nature of the fresh mix. Consequently after placement of concrete and at the onset of hardening, the region close to the aggregate surface is virtually devoid of cement grains but rather filled with water. This causes local micro-solution-filled pores (local regions of higher water-cement ratios) to occur in the vicinity of the aggregate particles. As hydration progresses, the voids in the transition zone are not effectively filled with cementitious reaction products due to the nature of cement reaction process (the reaction products are deposited at the surface of the cement particles). This leads to the formation of a more open and porous paste than the bulk matrix. Also, owing to the higher water-cement ratio at the interface and the relatively large amount of pore space, transportation of Ca^{2+} ions from the bulk cement paste to the interfacial zone is facilitated. At the paste-aggregate interface, crystallization conditions are more favourable than in the bulk cement paste. Thus, in the vicinity of the aggregate particles, crystalline hydration products, consisting essentially of calcium hydroxide and ettringite are easily formed.

One of the means that may be adopted to improve the microstructure of the interfacial zone is by use of good quality pozzolans and latent hydraulic binders (that is, pozzolans and hydraulic binders with "good" chemical composition) in conjunction with portland cement. Most of the particles of such materials should be finer than the cement particles so that they can fill the pores at the interface of the aggregate particles and between the cement grains. This effect will tend to reduce micro-bleeding and improve the density of the cement paste. Alternatively, blended cements, such as blastfurnace slag cement (with a high amount of slag as in portland blast furnace slag cement) and fly ash cement (containing $\approx$ 20–25% by mass of fly ash) may also be used. These suggestions are based on the fact that such materials tend to fill pores (as explained above); they also reduced surface and micro-bleeding in concrete and possess the ability to react with calcium hydroxide to produce additional cement gel.

4 Effects of the Interfacial Zone on Diffusion of Ions in Concrete

4.1 *Introduction*

This chapter examines the role of the cement paste-aggregate interfacial zone on diffusion of ions in concrete. In order to avoid the influence of the large aggregate particles, portland cement pastes and mortars were used. The water-cement ratio of the mixes was 0.40. Information from this study was used together with data from total porosity and pore size distribution measurements (see Section 3.5) to examine whether or not the interfacial zone influences the diffusion process.

4.2 *Chloride and Sodium Diffusion*

The rates of diffusion of Cl^- and Na^+ ions in 10-day old specimens with water-cement ratio (w/c) = 0.40 and sand-cement ratios of 0 and 1.0 are presented in Figs. 4.1 and 4.2 respectively. The results show that diffusion of Cl^- and Na^+ ions is more rapid in the plain cement paste, OPCP, than the corresponding mortar, OPCM. If, however, the data are considered on the basis of the paste volume in the mortar, OPCMP, then the diffusion process is faster in this paste than in the same volume of paste without sand, OPCP. The data in Figs. 4.1 and 4.2 indicate that in the presence of the sand particles, ionic diffusion through hardened cement paste increases. Using the slopes of the plots in Fig. 4.1 for Cl^- and Fig. 4.2 for Na^+, in combination with Equation 4 (Section 2.2.6), the diffusion coefficients, D_i for OPCP, OPCM, and OPCMP were calculated. The results are presented in Table 3.1.

Table 4.1 Coefficient of diffusion, D_i of ionic species in 10-day old pastes and mortars (OPCP = paste; OPCM = mortar; OPCMP = "normalized" paste in mortar)

	D_i $(m^2/s) \cdot 10^{-12}$		
Ionic species	OPCP	OPCM	OPCMP
Cl^-	1.3	1.2	1.9
Na^+	1.6	2.2	3.4

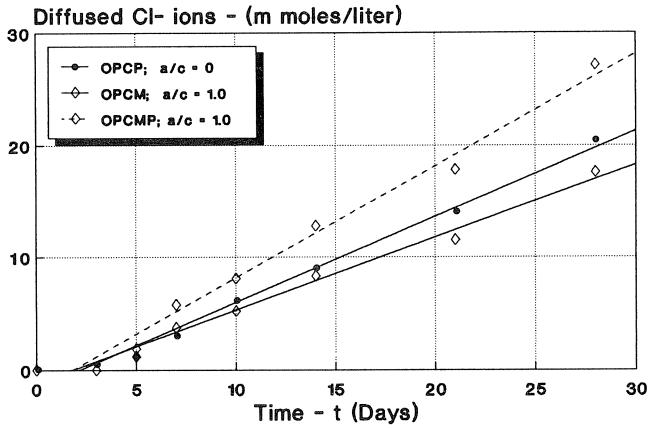

Fig. 4.1. Rate of diffusion of Cl^- ions in ordinary portland cement pastes and mortars (w/c = 0.40; a/c = 1.0; age: 10 days at start of test).

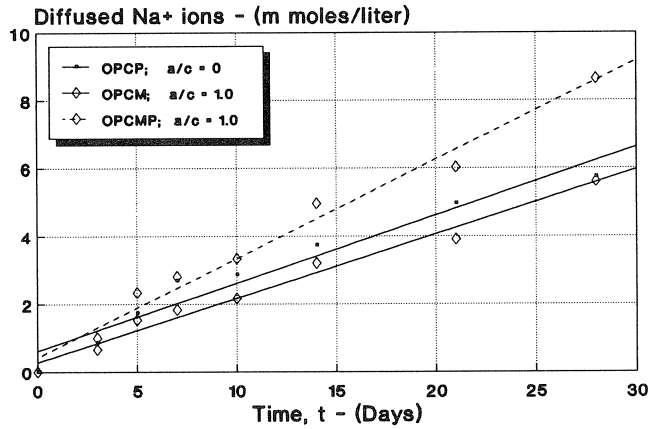

Fig. 4.2. Rate of diffusion of Na^+ ions in ordinary portland cement pastes and mortars (w/c = 0.40; a/c = 1.0; age: 10 days at start of test).

From the table it follows that the rate of diffusion of Cl^- and Na^+ ions through a 10-day old "mortar paste", OPCMP, is nearly 1.5 times (that is, $\approx 50\%$) faster than the corresponding paste without sand, OPC. The modification in the rates of diffusion in the mortars is likely to be due to the formation of a more permeable interfacial material around the aggregate particles.

4.3 *Discussion*

The modification of the ionic diffusion in the mortars as a function of sand-cement ratio appears to arise from cement paste-sand interfacial effects; it may be explained as follows. As the sand volume in the mortar increases, the number of particles of the sand,

and for that matter, the number of interfacial zones formed per unit volume of mortar also increases. Thus, when all the volumes of the interfacial regions formed around the sand particles are summed up, the total amount obtained per unit volume of mortar sample, that is:

(VOLUMEinterface / VOLUMEmortar)

is increased. In other words, as the volume of aggregate in the mortar increases, there will be a gradual predominance of the microstructural characteristics of the interfacial zone over those of the bulk paste. Thus, if the interfacial zone around the sand particles in the mortars is found to have a more permeable character, then it follows that, with increasing sand content, the mortar paste will be more permeable.

From the results of the pore size distribution studies it was observed that the increase in sand-cement ratio from 0 to 2 was accompanied by an increase in capillary porosity by a factor of 70. This effect (that is, the higher capillary porosity), is likely to be one of the characteristics of the interfacial zone. Scrivener et al. [18] using backscattered electron imaging combined with quantitative image analysis found relatively higher proportion of larger pores ($r > 0.1$ μm) at the transition zone than in the bulk paste. Uchikawa et al. [90] and Feldman [89] attributed the formation of such coarse pores ($r > 0.1$ μm) in mortars and concrete to interfacial effects. Similar conclusions were drawn by Nyame [30].

The results of this study show that the interfacial zone is more porous than the bulk cement paste matrix. However, considering the OPCMP/OPCP factors obtained from the simple mathematical normalization of the diffusion data (OPCMP/OPCP = 1.5 to 2.0) in comparison with the much larger increase in capillary porosity, then the role of the interface on the diffusion of ions in concrete can be considered to be relatively minor. The results of the study suggest that ionic diffusion processes in concrete are controlled mainly by the cement paste matrix which can be understood by realizing that the bulk paste matrix is the only continuous phase; the interfacial zones are isolated from each other by volumes of the bulk paste.

4.4 *Concluding Remarks*

Although it was found from the porosity and pore-size distribution studies that the cement paste-aggregate interfacial zone is more porous than the cement paste matrix, mathematical analysis of the data from Cl^- and Na^+ ion diffusion in the pastes and mortars with the same mix design and curing conditions, points to the fact that the paste-aggregate interfacial zone plays a minor role in the diffusion of ions in concrete. The results suggest that in normalweight concrete the paste matrix is the continuous phase and is mainly responsible for ionic diffusion processes.

5 Effects of Mineral Additives on the Cement Paste-Aggregate Interfacial Zone in Concrete

5.1 *Introduction*

This chapter summarises the results of a study that was aimed at examining the effect of various mineral additives on the cement paste-aggregate interfacial zone. The mineral additives in question are: a thermally activated kaolinite (MK), a silica fume (SF), three types of pulverised fuel ash and a ground granulated blast furnace slag as part of portland blast furnace slag cement (PBFSC) with about 65–70% by mass of slag as partial replacement of the portland cement klinker. The characteristics of these materials together with the mix compositions and the experimental procedures are given in Chapter 2. The results obtained for the three fly ashes used were similar. For this reason the data for only one of them (EFA) have been presented.

5.2 *Effects of the Mineral Additives on $Ca(OH)_2$ Evolution*

Fig. 5.1 shows the effects of the mineral additives on the evolution of calcium hydroxide ($Ca(OH)_2$) in portland cement mortars. The rate of development of $Ca(OH)_2$ in the blended mortars was used as a measure of the extent of the pozzolanic reaction in the mortars. The reaction of silica fume with $Ca(OH)_2$ appears to start early; by 90 days of hydration most of the $Ca(OH)_2$ produced had reacted. Apparently, the fly ash reacts less rapidly than the silica fume. It is interesting to note that for hydration periods up to about 28 days the $Ca(OH)_2$ content of the fly ash mix increased. This suggests that during this stage of hydration, most of the ash particles did not react with the $Ca(OH)_2$ liberated from the cement hydration. Apparently up till this age, the ash appears to behave as an inert filler. SEM examinations reveal that most of the ash particles, particularly the larger ones, tend to act as as micro-aggregate particles which serve as

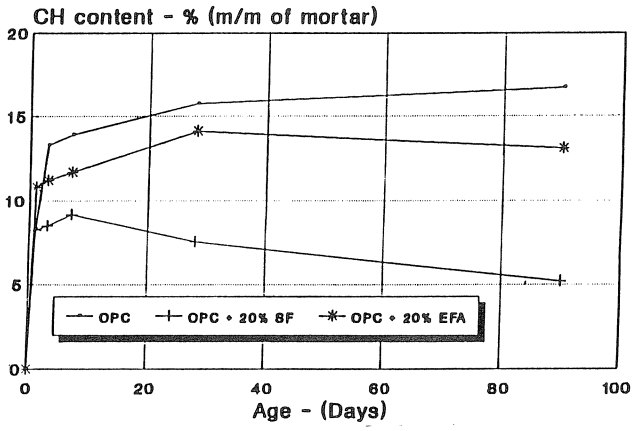

Fig. 5.1. Effects of fly ash and silica fume on the evolution of calcium hydroxide in portland cement mortars.

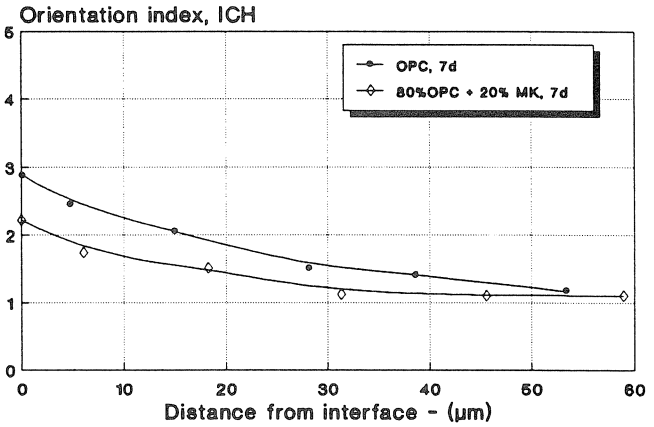

Fig. 5.2. Effects of addition of metakaolinite on the degree of orientation of calcium hydroxide at the cement paste-granite interfacial zone (age: 7 days).

preferential sites for precipitation of $Ca(OH)_2$ (Fig. 5.2). The study also revealed that most of the calcium hydroxide crystals remain in intimate contact with some of the ash particles even after six months of hydration.

5.3 *Effects of the Mineral Additives on the Interfacial Zone*

As described before, the XRD analysis showed a pronounced effect of the degree of orientation of calcium hydroxide crystals at the (OPC)cement paste-coarse aggregate interfacial zone. The effects of various mineral additives are discussed below.

5.3.1 Effects of Metakaolinite

The effect of addition of metakaolinite on the orientation index, I_{CH} is shown in Figs. 5.2 and 5.3 for 7- and 100-day old composite specimens. The water-binder ratio of the mixtures was 0.40. It is clear from the two figures that for both ages, the addition of metakaolinite decreased the relative amount and the degree of orientation of the calcium hydroxide at the vicinity of the aggregate. It is also interesting to note that the thickness of the interfacial zone decreased from about 40 μm at 7 days to less that 10 μm at 100 days of hydration, as compared to 40 to 50 μm for the ordinary portland cement paste at 7 and 100 days respectively.

5.3.2 Effects of Blast Furnace Slag

Fig. 5.4 shows the effect of age on the maximum orientation index value, $I_{CH(max)}$ for OPC and PBFSC. The $I_{CH(max)}$ value is the orientation index value immediately after debonding of the paste from the aggregate, that is prior to grinding. For all the speci-

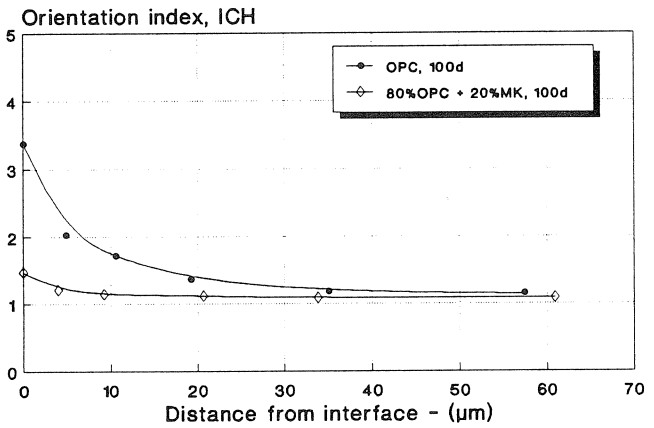

Fig. 5.3. Effects of addition of metakaolinite on the degree of orientation of calcium hydroxide at the cement paste-granite interfacial zone (age: 100 days).

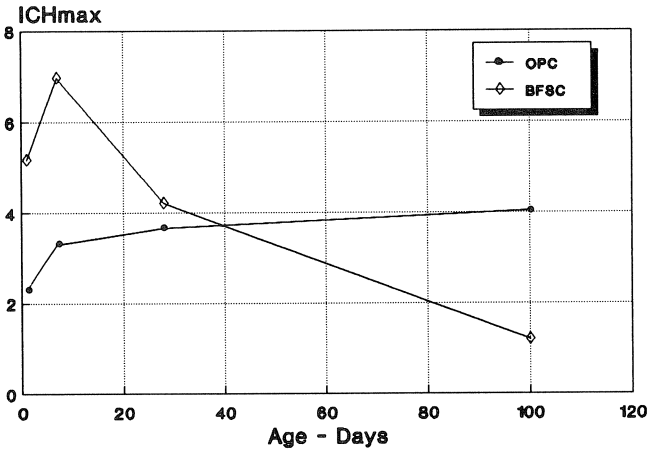

Fig. 5.4. Effect of age on the maximum degree of orientation of $Ca(OH)_2$ at the paste-granite interfacial zone for OPC and PBSFC pastes.

mens studied, this first I_{CH} value was the highest, hence the designation $I_{CH(max)}$. Up to about 28 days the amount of calcium hydroxide and the orientation index values at the interfacial zone are higher for PBFSC than for OPC. The graph, however, shows that after about 7 days, the orientation index values for PBFSC tend to decrease. This suggests a possible reduction in the amount of calcium hydroxide at the interfacial zone possibly resulting from the reaction between the slag and calcium hydroxide (see also Section 5.2). It could also mean that as a consequence of the hydraulic action of the slag, after about 7 days of hydration the interfacial layer becomes densified, in which case the ease of transport of Ca^{2+} and OH^- ions to the interface for crystallization of $Ca(OH)_2$ at the interface became reduced. Portland blast furnace slag cements and ordinary port-

land cement containing slags as partial cement replacements are known to form a more discontinuous pore structure with an impermeable cement paste system than ordinary portland cement pastes (9, 10).

Figs. 5.5 and 5.6 show the distribution of I_{CH} at the interfacial zone for OPC and PBFSC at ages of 1 and 7 days respectively. Relative to the ordinary portland cement, the much finer portland blast furnace slag cement showed a decrease in the thickness of the interfacial zone.

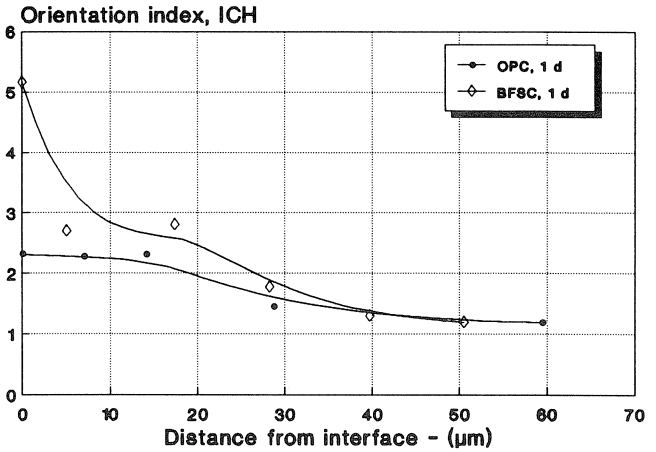

Fig. 5.5. Degree of orientation of $Ca(OH)_2$ at the paste-granite interface in portland blast furnace slag cement paste system (age: 1 day).

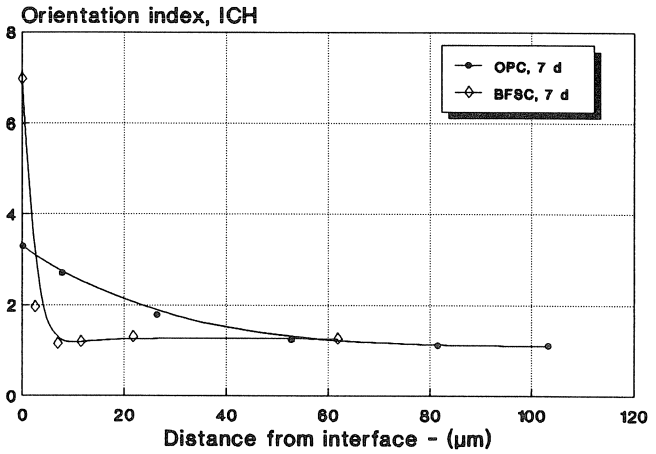

Fig. 5.6. Degree of orientation of $Ca(OH)_2$ at the paste-granite interface in portland blast furnace slag cement paste system (age: 7 days).

5.3.3 Effects of Silica Fume and Fly Ash

The effects observed on the paste-aggregate interfacial zone for metakaolinite and blast furnace slag in the foregoing sections have also been observed for composites containing SF and EFA. Using Figs. 5.2 and 5.3 for metakaolinite and similar data for EFA and SF, the orientation index, I_{CH}, and the thickness of the interfacial zones, δ, for various composites at specified ages were calculated. The results are presented in Tables 5.1 and 5.2. From the data in Table 5.1 and 5.2, the following deductions can be made:

a. with increasing age, the values of the orientation index, I_{CH}, *increased* for the reference mix, and *decreased* for the blended composites; this suggests a decreasing content of $Ca(OH)_2$ at the interface, which possibly resulted from the pozzolanic reaction of the blending materials;
b. at 7 days, the I_{CH} values of the blended mixes were lower than those of the plain mixes; but the thickness of the paste-aggregate interfacial zones of the blended mixes were approximately the same as those of the reference mixes; this suggests that at 7 days of hydration there was some pozzolanic reactivity of the blending materials, but not enough to cause appreciable densification and reduction of the thickness of the transition zone;
c. as the curing period increased, the thickness of the interfacial zones of the reference mixes remained nearly the same, although the I_{CH} values increased; for the blended mixes, the interfacial zones became thinner, and the I_{CH} values decreased further; this suggests that in the blended composites, as curing progressed, there was gradual densification of the interfacial layer probably by conversion of $Ca(OH)_2$ at the interface (by the pozzolanic reaction) into secondary C–S–H and other hydrates – a kind of an *"elimination-by-substitution"* reaction.

Table 5.1 Maximum orientation index of $Ca(OH)_2$ crystals I_{CHmax}, and thickness of the interfacial zone, δ for cement paste-granite composites after 7- and 100 days of curing for water-solids ratio of 0.40

Age of the specimens	OPC	80% OPC + 20% MK
7 days:		
orientation index, I_{CHmax}	2.9	2.0
thickness, δ (μm)	49.4	39.7
100 days:		
orientation index, I_{CHmax}	3.4	1.5
thickness, δ (μm)	43.0	9.8

From Tables 5.1 and 5.2 it implies that, as the curing period increased, there was transformation of the weak, porous, and permeable interfacial region into a more compact and impermeable layer. The decrease in the thickness of the transition zone of the blended mortars means that the volume of the more permeable region which may be used as a preferential path for transport of fluids is also reduced. Accessibility of such mortars to fluids is likely to be decreased.

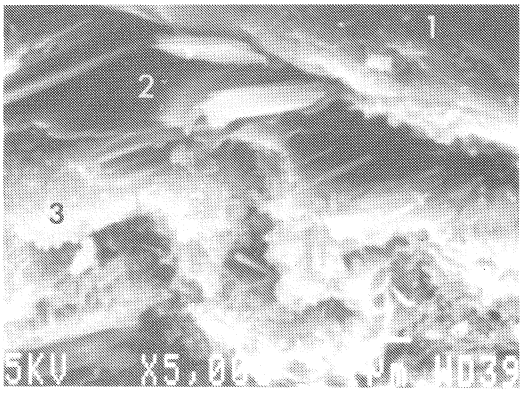

Fig. 5.7. SEM photo of a fractured surface of OPC (reference) mortar showing the microstructure of the paste-aggregate interface; 1 = aggregate; 2 = $Ca(OH)_2$ crystals; 3 = paste (age: 7 days).

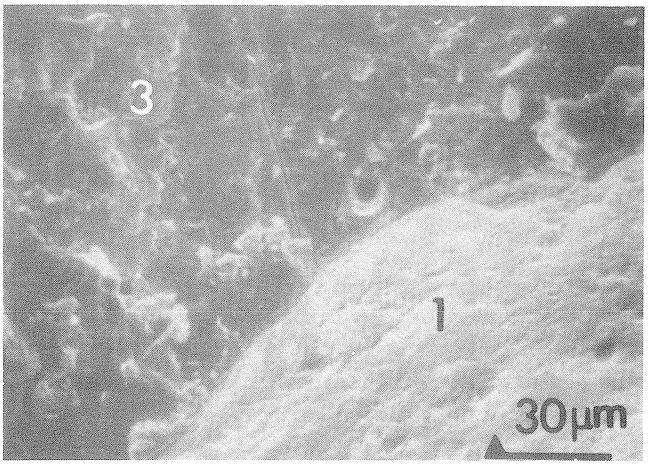

Fig. 5.8. SEM photo of a fractured surface of portland cement mortar containing silica fume showing the microstructure of the cement paste-aggregate interfacial zone; 1 = aggregate; 3 = paste (age: 28 days).

hardness distribution and, for that matter, the homogeneity of the paste. The improvement in the microstructure at the interfacial zone of the microsilica blends is attributed to the improved grain packing and reduced micro-bleeding at the aggregate particle interface soon after formulation of the mix. These physical effects laid the "platform" for further pore structural improvements through the cementation of the solids together with the extra C–S–H gel produced from the pozzolanic reaction between the microsilica and the calcium hydroxide at the paste-aggregate interface.

Table 5.2 Maximum orientation index of $Ca(OH)_2$ crystals I_{CHmax}, and thickness of the interfacial zone, δ for cement paste-granite composites after 7-, 28- and 100 days of curing for water-solids ratio of 0.40 (the data in brackets were obtained using polypropylene plastic plate as a "model coarse aggregate"; n.d. = not determined)

Age of the specimens	OPC	80% OPC + 20% EFA	80% OPC + 20% SF
7 days:			
orientation index, I_{CHmax}	3.3 (5.0)	(3.8)	2.5
thickness, δ (μm)	53.8 (54.5)	(39.0)	50.9
28 days:			
orientation index, I_{CHmax}	3.6 (5.9)	(2.2)	2.0
thickness, δ (μm)	32.7 (51.4)	(9.4)	20.0
100 days:			
orientation index, I_{CHmax}	4.0	n.d.	1.8
thickness, δ (μm)	50.3	n.d.	7.3

5.4 *SEM Studies on the Cement Paste-Aggregate Interface*

SEM studies with microprobe analyses showed that in the case of mortars with additions of silica fume, metakaolinite and portland blast furnace slag cement, calcium hydroxide which initially crystallized at the interface disappeared later on when pozzolanic reaction had occurred as shown for instance in Figs. 5.7 and 5.8. During the first few days $Ca(OH)_2$ crystals were found with aid of the SEM at the paste-aggregate interface for both the reference mix and the mix containing the mineral additives. In the case of the fly ash mix, for example, some of the ash particles themselves acted as "inert fillers" by providing nucleation sites for $Ca(OH)_2$. This nucleating effect is known to occur for similar finely-divided mineral additives, such as silica fume and metakaolinite. After the pozzolanic reaction has advanced, the interfacial layer becomes denser with practically no visible large crystals of calcium hydroxide, as shown in Figs. 5.7 and 5.8. In general, a more compact interface was observed when these materials are used in combination with ordinary portland cement.

The significantly reduced amount of calcium hydroxide at the interfacial region will decrease the buffer of hydroxyl, OH^- ions. Also, the densification and the "thinning" of the interfacial region is likely to reduce the penetration rate of aggressive ions into the concrete.

5.5 *Microhardness Studies on the Cement Paste-Aggregate Interface*

The results with limestone rock composite are presented in Fig. 5.9. The data show that the hardness of the interfacial zone was substantially increased by addition of silica fume if compared with ordinary portland cement paste of the same water-to-binder ratio. The "trough" or "valley" formed at the aggregate interface in the reference paste is substantially flattened by addition of 20% (by mass) of silica fume. The addition of the silica fume as partial portland cement replacement tended to homogenize the micro-

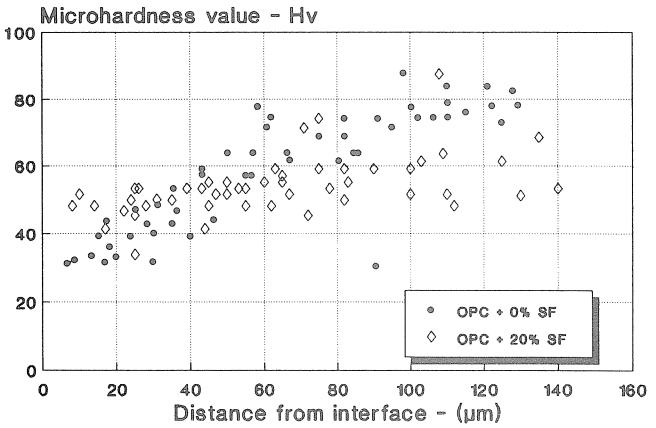

Fig. 5.9. Effects of partial portland cement replacement by silica fume on the microhardness of the transition zone between paste and limestone rock used (28 days old).

6 Influence of Pozzolans on the Interfacial Zone in Relationship to the Transport of Water and the Diffusion of Ions in Concrete

6.1 *Introduction*

This chapter examines the influence of three pozzolans on the cement paste-aggregate interfacial zone in relation to water loss from concrete and diffusion of ions in concrete. The data were obtained from the kinetics of moisture movement from mortars and the rates of diffusion of Cl^-, Na^+ and K^+ ions in mortars. Pore structural studies from mercury intrusion porosimetry and information from Chapter 5 were used to support the analysis and the interpretation of the data obtained in this chapter.

6.2 *Pore Structure*

Fig. 6.1 shows the rates of drying curves for the 100-day old mortars, dried in an oven at 40 °C. The mortars containing the pozzolans tend to dry at a slower rate than the plain mortar. This effect is most pronounced in the case the silica fume mortar, SFM, and least remarkable with the fly ash mortar, EFAM. The effect is probably due to the occurrence of cement pastes with a lot more finer, more tortuous and less accessible pores in the mortars containing the pozzolans than the cement paste in the plain mortar.

The mercury intrusion porosity curves for OPCM, MKM and EFAM after 100 days of curing are presented in Fig. 6.2. The data for the silica fume mortar were comparable to the data obtained for metakaolinite. For this reason only those for the metakaolinite are presented. The results show that the reference mortar has the highest total mercury intrusion porosity at 100 days of hardening.

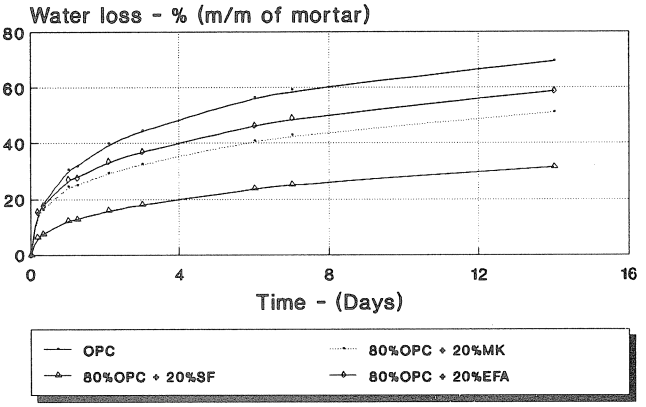

Fig. 6.1. Rate of loss of water from mortars with and without pozzolans (w/s = 0.40; a/c = 1.0; age = 100 days).

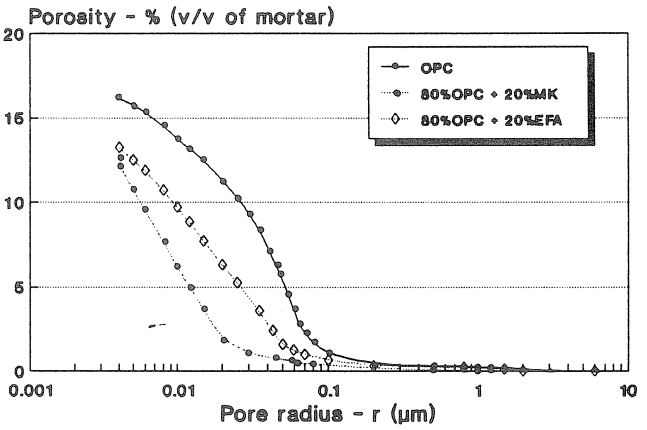

Fig. 6.2. Pore size distribution of mortars plotted as volume percent of mortar (w/s = 0.40; a/s = 1.0; age = 100 days).

The data also show that MKM is denser than EFAM. Of the three mortars, the reference mortar (containing no pozzolanic addition) OPCM, has the highest capillary pore volume, followed by EFAM and MKM.

Scrivener et al. [18] using backscattered electron imaging combined with quantitative image analysis found relatively higher proportion of larger pores ($r > 0.5$ μm) at the transition zone than in the bulk paste. Uchikawa et al. [90] and Feldman [89] attributed the occurrence of coarser pores ($r > 0.5$ μm) in mortars and concrete to the porous character of the paste-aggregate interfacial zone. The lower capillary pore volume of EFAM and MKM suggests that the paste-sand interfacial zones of these mortars have been densified. It also suggests that the pores in the paste matrix are smaller. The densification may have resulted partly from:

(i) the improved particle packing of the cementitious materials in the blended mortars, especially at the paste-sand interfaces ([83]; see also Chapter 5), and partly from

(ii) the deposition of secondary hydrates arising from the pozzolanic reaction between the blending components [see Chapter 5].

6.3 *Diffusion of Cl^-, Na^+ and K^+ Ions*

The kinetics of diffusion of Cl^- in the mortar specimens are illustrated in Fig. 6.3. It is evident from Fig. 6.3 that the blended mixes offer a higher resistance to the diffusion of Cl^- ions in the mortars. Using the slopes of the plots in Fig. 6.3 for Cl^- and similar data from graphs plotted for Na^+ and K^+, the coefficients of diffusion, D_i, of the ions were determined. The results and other relationships are presented in Tables 6.1 and 6.2.

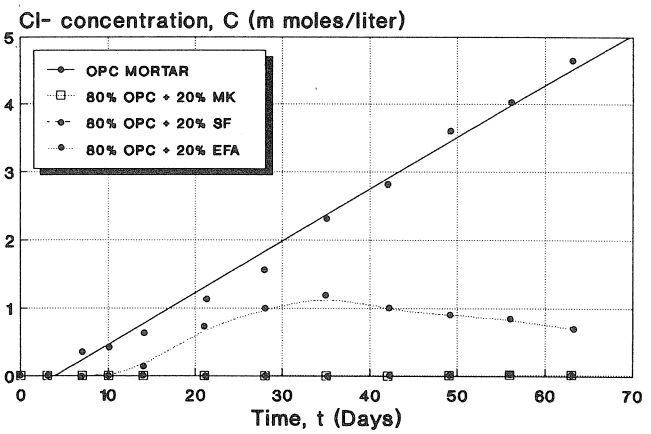

Fig. 6.3. Rate of diffusion of Cl^- ions in mortars with and without pozzolans (w/s = 0.40; a/s = 1.0; age: 100 days at start of test).

Table 6.1 Coefficient of diffusion of ionic species in portland cement mortars with and without silica fume or metakaolinite

	D_i ($m^2 \cdot s^{-1}$) $\cdot 10^{-13}$		
Ionic species	OPCM	MKM	SFM
Cl^-	5.97	0.10	0.11
Na^+	1.88	0.03	0.03
K^+	2.59	0.07	0.06

Table 6.2 Ratio of D_i of OPCM to D_i of the pozzolans

Ionic species	D_i OPCM/D_i OPCM	D_i OPCM/D_i MKM	D_i OPCM/D_i SFM
Cl^-	1	60	55
Na^+	1	63	63
K^+	1	37	43

It can be seen that:

(i) The use of the the pozzolans in combination with ordinary portland cement tends to increase the resistance of the mortars to diffusion of Cl^-, Na^+ and K^+ ions. For example, the diffusion of Cl^- ions in the 100-day old plain mortar at 20 °C is sixty times as fast as the rate of diffusion of Cl^- ions in the MK or the SF mortars.

(ii) The metakaolinite (MK) and the silica fume (SF) appear to be more effective than the Class F fly ash (EFA) in limiting the diffusion of ions in the mortars. The diffusion rate in the case of EFA decreases with time indicating the slow pozzolanic reaction which is typical of most Class F fly ashes [83].

The results of this study are in agreement with the work of Page et al. [85], Collepardi et al. [91], Dhir et al. [87], Sturrup and Hooton [92], Uchikawa et al. [90], and Sarkar and Aitcin [73].

6.4 *Discussion*

In Chapters 3 and 4, it was found that the interfacial zone in portland cement mortars greatly increased capillary porosity relative to pure portland cement pastes, but had a relatively small effect on the transport of fluids. It was suggested that the cement matrix, as a continuous phase, controlled the transport processes in concrete. Although the interfacial zone was found to be significantly more porous than the bulk cement paste, it was found to play only a relatively small role in the transport processes in concrete. This is presumably because the large pores at the interfacial zones are not interconnected with each other but rather the relatively small pores of the matrix.

Since in the blended cement mortars, there is a substantial decrease in the rate of transport of water and the diffusion of Cl^-, Na^+ and K^+ ions this marked decrease in the transport capacity must be due to the improvement in the microstructure of the cement matrix.

The ionic diffusion results in Chapter 4 also show that only a factor of 1.3 to 2.0 is obtained when the diffusion of ions in the plain ordinary portland cement pastes was compared to that of the mortar specimens that were investigated. The "continuous phase", which was found to control the diffusion processes was found to be the bulk cement paste matrix. In this study, however, the data in Table 6.2 show that in the presence of silica fume or metakaolinite, a factor of $\approx$ 35–60 is obtained when the diffusion process in the plain mortar mix is compared to the SF or MK mortar mixes. These high ratios are obtained regardless of the fact that the thickness of the paste-aggregate interfacial zone in these systems is not "zero" as shown in Tables 5.1 and 5.2.

Therefore the increased resistance of the blended cement mortars against penetration of aggressive ions must be due in part to the improvement of the microstructure of the paste-aggregate interfacial layer, but more importantly, to the marked improvement or the densification of the matrix of the blended mixes. This observation is in agreement with the results of Malek and Roy [62], who concluded after a similar study that the diffusion process of chloride in concrete is mainly controlled by the composition of the cementitious matrix.

6.5 *Concluding Remarks*

The influence of pozzolans on the paste-aggregate interfacial zone in relationship to the loss of water from mortars and the diffusion of Cl^-, Na^+ and K^+ ions in mortars has been studied. On the basis of the results presented in this paper, the following conclusions can be drawn. Addition of the pozzolans, MK, SF and EFA to portland cement as partial cement replacement inhibited the rates of diffusion of Cl^-, Na^+ and K^+ ions in the mortars and reduced the rate of loss of water from the mortars.
These substantially improved effects of the pozzolans must be mainly due to improvement in the permeability of the bulk cement paste matrix because the improved effects are more pronounced when plain ordinary portland cement mortars and blended cement mortars are compared than when plain cement paste and plain mortar are compared.

7 Effects of Silica Fume and Metakaolinite on the Interfacial Zone with Respect to the Strength of Mortars

7.1 *Introduction*

Silica fume and metakaolinite have been shown to improve the microstructure of cement paste in concrete by densifying the cement paste matrix and the porous paste-aggregate interfacial zone (see Chapter 5). These beneficial effects have been shown to result in a pronounced increase in the resistance of concrete to penetration of aggressive compounds (see Chapter 6). In this chapter, the role of these two pozzolans on the cement paste-aggregate interfacial zone in relationship to the compressive strength development of portland cement mortars are examined.
Portland cement pastes and mortars containing 0 and 20% (by mass) of silica fume or metakaolinite with water-to-binder ratios of 0.40 and 0.50 were used for the study.

7.2 *Plain Mixes*

Figs. 7.1 and 7.2 show the compressive strength development of plain portland cement (OPC) pastes and mortars as a function of age. Although the sand particles are stronger than the cement pastes, the results in these two figures show that the plain pastes are comparatively stronger than the corresponding mortars.

7.3 *Mixes Containing Silica Fume or Metakaolinite*

The influence of silica fume or metakaolinite on the compressive strength development of cement pastes and mortars is illustrated in Figs. 7.3, 7.4 and 7.5. There is essentially no difference in the strength development between the SF or the MK pastes on the one hand and the plain cement pastes on the other hand as shown in Figs. 7.3 and 7.4.

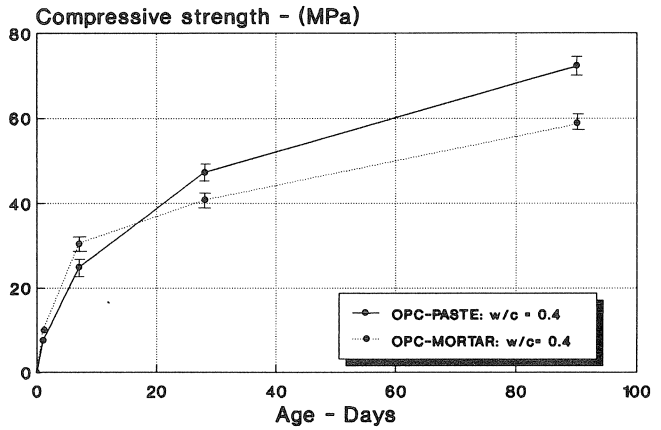

Fig. 7.1. Compressive strength development of plain OPC cement pastes and mortars as a function of age (w/c=0.4; specimens cured in a fog room at 20°C in lime-saturated solutions).

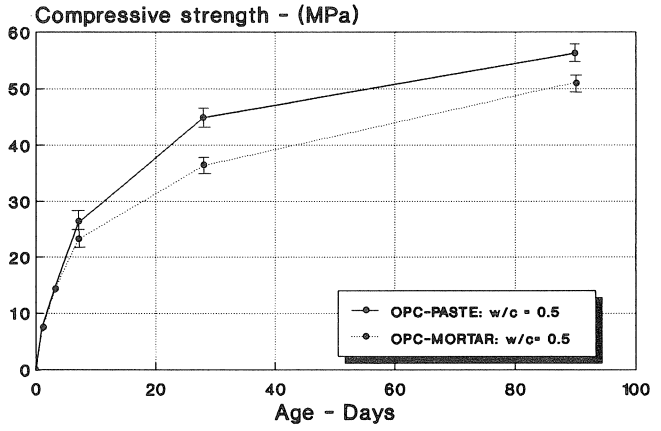

Fig. 7.2. Compressive strength development of plain OPC cement pastes and mortars as a function of age (w/c=0.50; specimens cured in a fog room at 20°C in lime-saturated solutions).

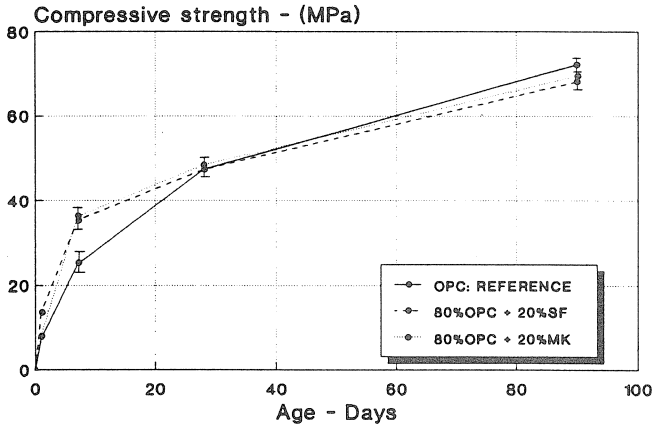

Fig. 7.3. Effects of addition of SF and MK on the compressive strength development of portland cement pastes (w/s = 0.40; specimens cured in a fog room at 20°C in lime-saturated solutions).

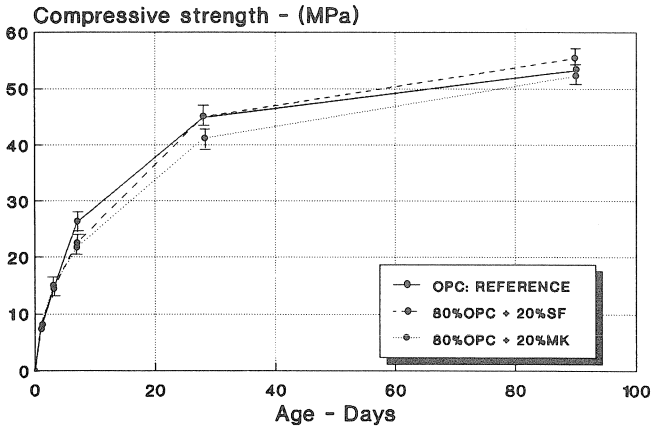

Fig. 7.4. Effects of addition of SF and MK on the compressive strength development of portland cement pastes (w/s = 0.50; specimens cured in a fog room at 20°C in lime-saturated solutions).

Quite contrasting, it is evident from Figs. 7.5 and 7.6 that the silica fume and metakaolinite mortars display higher compressive strengths than the corresponding plain mortars. This higher strength development is already observed as early as one day after the formulation of the mortars. The results also show that there is virtually no difference between the compressive strength of the SF mixes and the MK mixes. For that matter subsequent discussion of the compressive strength data will be confined to the silica fume.

A comparison of the compressive strength development of mortars and pastes containing 0 and 20% silica fume at w/s = 0.40 is presented in Figs. 7.1, 7.2, 7.7 and 7.8. Figs. 7.1 and 7.2 represent the plain mixes and Figs. 7.7 and 7.8 the silica fume blends. With

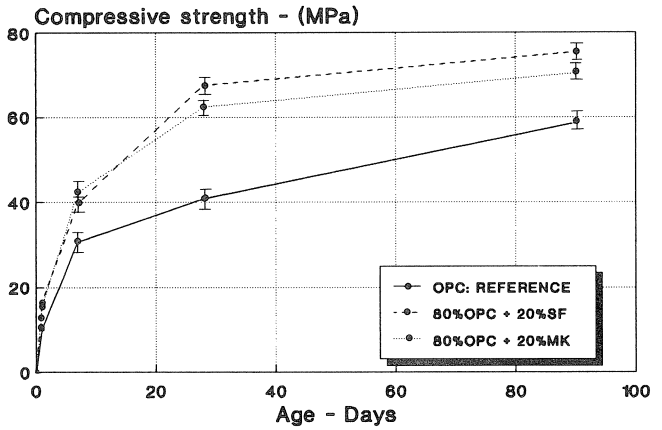

Fig. 7.5. Effects of addition of SF and MK on the compressive strength development of portland cement mortars (w/s=0.40; specimens cured in a fog room at 20°C in lime-saturated solutions).

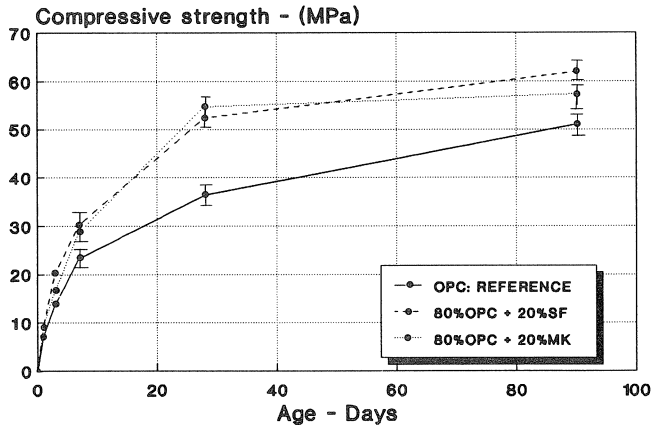

Fig. 7.6. Effects of addition of SF and MK on the compressive strength development of portland cement mortars (w/s=0.50; specimens cured in a fog room at 20°C in lime-saturated solutions).

no silica fume, the paste is relatively stronger than the mortar. In contrast to that, the mixes containing silica fume show a reverse trend. The mortars are comparatively stronger than the pastes.

This increase in compressive strength at 1 day for the SF and MK blends is probably due to the improved solids packing of the cement grains ($\approx$ 10–30 μm in diameter) and the SF or MK particles ($\approx$ 0.1 μm and 1.4 μm average diameter respectively) and the reduced micro-bleeding at the paste-aggregate interface (see Chapters 5 and 6). The increase in the rate of cement hydration is also likely to contribute to the early adhesive

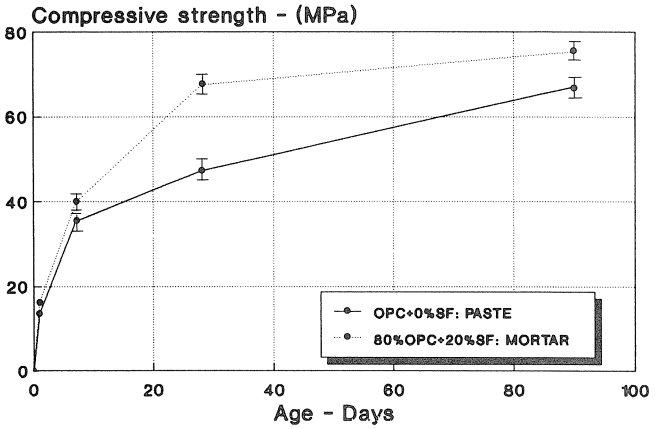

Fig. 7.7. A comparison of the compressive strength development between silica fume pastes and mortars (w/s = 0.40; specimens cured in a fog room at 20°C in lime-saturated solutions).

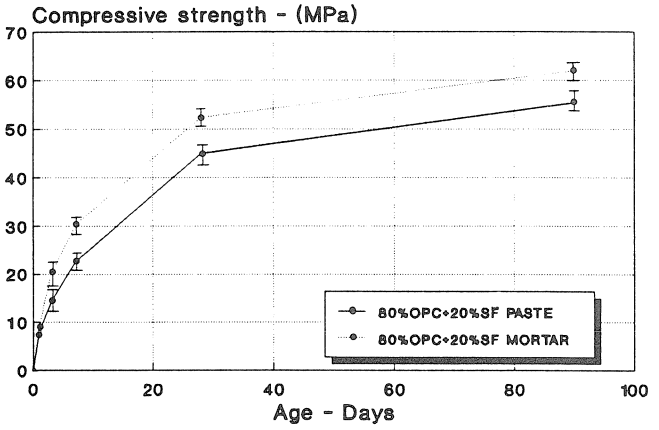

Fig. 7.8. A comparison of the compressive strength development between silica fume pastes and mortars (w/s = 0.50; specimens cured in a fog room at 20°C in lime-saturated solutions).

strength development of the cement paste to the aggregate particles [83]. Subsequent increase in adhesive strength is probably due to the production of C–S–H gel through the pozzolanic reaction between the SF or MK and the CH produced from the cement hydration.

7.4 *Discussion*

Theoretically, two effects may have contributed to the observed improvement in the strength of mortars when silica fume and metakaolinite were used in conjunction with portland. These are:

1. Improvement of the interfacial zone: this is brought about by the better particle packing and the pozzolanic reaction which result in the formation of a denser and a stronger mortar.
2. Improvement of the bulk paste matrix: also brought about by better particle packing and the pozzolanic reaction which also result in the formation of a denser and a stronger mortar.

From the results of the present study, the improvement of the strength of the mortars in the presence of SF and MK cannot be due to effect "2" above, that is, the improvement of the bulk cement paste matrix because no differences between the compressive strength of the plain OPC pastes and the OPC-SF or OPC-MK pastes were observed although differences were observed in permeability, pore size distribution and capillary porosity (see Chapter 6). Therefore the effect on compressive strength must be due to improvement of the interfacial zone.

From the above discussion, the lower compressive strength development of the portland cement mortars compared to their corresponding cement pastes (Figs. 7.1 and 7.2) is likely to be due to interfacial effects which result in a less effective transfer of stress from the cement matrix to the aggregate particles. This observed effect is in agreement with the work of Powers [93] (presented in Fig. 7.9) which shows that for the same gel-space ratio (the gel/space ratio is the ratio of the solid products of hydration to the space available for these hydration products; in other words, the gel/space ratio is a representation of the capillary porosity of the cement paste), the presence of sand particles tends to lower the compressive strength of cement pastes. Powers attributed this effect to inhomogeneities with respect to the elastic properties of mortar and to a modification of the mode of failure of cement pastes in the presence of sand particles.
When silica fume or metakaolinite is added to mortars as partial cement replacement, the interfacial zone becomes denser and thinner (see Chapter 5). This interfacial improvement leads to a better transfer of stress from the matrix to the sand particles. Since the sand particles are comparatively stronger (higher modulus of elasticity) than the matrix, this effect results in a higher compressive strength development of the SF or MK mortars compared to their corresponding pastes and to the plain OPC-mixes. The transfer of stress from matrix to aggregate (with a higher modulus of elasticity) is illustrated schematically in Fig. 7.10.

Other investigators have suggested other causes for the difference in effects of mineral additions on the strength of pastes and mortars. In [18, 89], it is suggested that in cement pastes, the ultrafine cementitious additions such as silica fume or metakaolinite ($> 5\%$ by mass of cement as solids) are not effectively dispersed even in the presence of superplasticizers and after prolonged period of mixing. For this reason, although cement hydration may be accelerated, because some of the particles exist as "clumps", complete dissolution of these clumps for subsequent pozzolanic reaction is not achieved. Only partial dissolution of the particles is achieved. In the mortars, however, the tumbling and shearing of the aggregate particles with the silica fume or metakaolinite

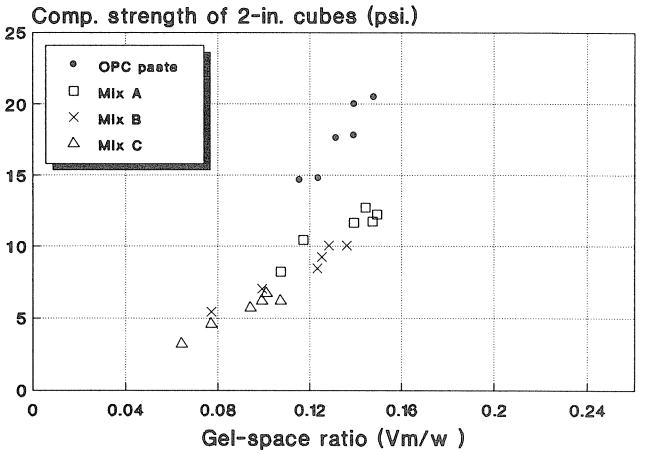

Fig. 7.9. Strength versus gel-space ratio of neat cement pastes and mortars (Redrawn from Powers [113]).

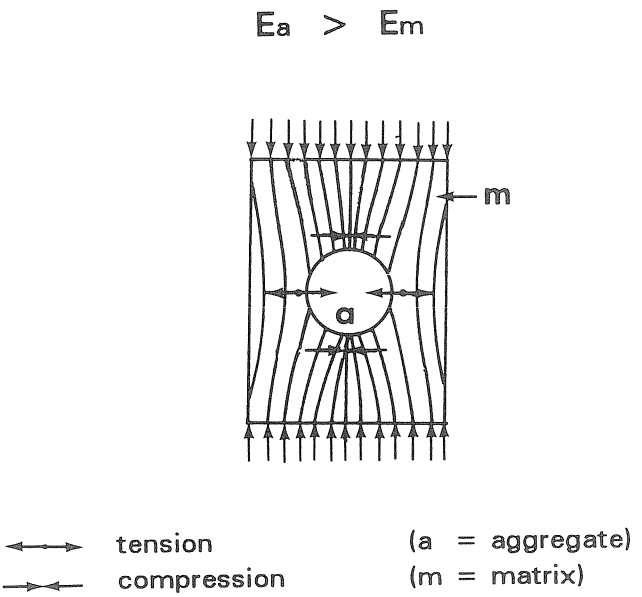

Fig. 7.10. Schematic representation showing the transfer of stress from matrix to aggregate under compressive load.

particles during the mixing process tend to break any "clumps" formed. In brief, the performance of these additions in pastes is according to these investigators limited due to inhomogeneous mixing.

7.5 *Concluding Remarks*

1. Addition of silica fume and metakaolinite increased significantly the compressive strength of mortars.
2. Silica fume and metakaolinite, however, did not show significant strengthening effects in cement pastes, at least, for the water-binder ratios considered in this study.
3. The increased strength of the silica fume and the metakaolinite mortars are believed to be due primarily to the thinner and more compact interfacial zone which improved the transfer of stress from the matrix to the aggregate particles.

8 Summary of Conclusions

The microstructural features of the transition zone between portland cement paste and aggregate particles in concrete are considerably different from those of the bulk matrix. The zone is less compact with a higher proportion of calcium hydroxide than the bulk matrix. The calcium hydroxide crystals have a preferential orientation in such a way that their *c*-axes are nearly perpendicular to the surface of the aggregate.
A higher density of fractures and microcracks occurs at the interfacial zone than in the bulk matrix. Most of the fractures tend to run directly along the paste-aggregate interface and along the cleavage planes of the calcium hydroxide crystals. The cement hydration products in the vicinity of the aggregate particles are loosely bonded to one another and to the aggregate particles. Compared to the aggregate particles and the bulk cement paste, the hardness value of the interfacial layer is the lowest. It is also the most porous component of concrete. Thus, in ordinary portland cement mortar or concrete, the interfacial layer between the bulk cement paste and the aggregate particles can be considered as a "weak link". On the average, the interfacial zone is ≈ 50 μm thick and occupies about 30 to 50 % of the total volume of cement paste in concrete.

Although the interfacial zone in ordinary portland cement concrete is more porous than the bulk cement paste, this study shows that it plays a minor role in the transport of water and the diffusion of ions in concrete. Considering the range of water-cement ratios used in this study, it is evident that water transport and diffusion of ions in concrete are very much controlled by the bulk cement paste matrix which is the only continuous phase in concrete. The diffusion of ions is influenced only to a minor extent by the porous interfacial zone.

Good quality pozzolans such as fly ash, silica fume, and metakaolinite, and latent hydraulic binders such blast furnace slag may be used in conjunction with ordinary portland cement to improve the structure of the interfacial zone. Alternatively, blended cements, such as blastfurnace slag cement ($\approx 70\%$ by mass of slag) and fly ash cement ($\approx 20\%$ by mass of fly ash) may be used to "reinforce" the weak microstructure of the paste-aggregate interfacial zone.
In general, the action of the pozzolans and blast furnace slag leads to the formation of a

denser interface, with reduced quantity and decreased crystal orientation of calcium hydroxide. There is also a decrease in the thickness of the interfacial zone. The study also shows that addition of pozzolans such as pulverised fuel ash, silica fume, and thermally activated kaolin to ordinary portland cement as partial cement replacement slows down the transport of aggressive agents in concrete. In particular:

a. the rates of diffusion of Cl^-, Na^+ and K^+ ions in mortars and concretes are reduced significantly;
b. the rate of loss of water from mortars and concretes also remarkably reduced by use of the pozzolans.

These effects have been shown to be mainly due to improvement in the pore size distribution of the bulk matrix and only to a minor extent to the improvement of the interfacial zone. In general, the reduced rate of transport of water, vapour and ions increases the resistance of concrete against sulphate attack. It is likely to decrease the vulnerability of concrete towards the destructive alkali-aggregate reaction (in the case of concrete containing reactive aggregates), and it improves the protection of steel reinforcement against chloride penetration.

The study also shows that for the same age, and with the same water-cement ratio, ordinary portland cement pastes have higher compressive strengths than their corresponding mortars. This effect is observable for all the mixes regardless of the fact that the sand particles are considerably stronger than the cement pastes.

The decrease in compressive strength with increasing water-cement ratio is ascribed to interfacial effects, namely, the heterogeneity and microstructural defects of the interfacial layer (higher density of microcracks, higher amounts of oriented calcium hydroxide, loosely-bonded cement hydration products, and the associated higher micro-porosity). Addition of silica fume or metakaolinite increases significantly the compressive strength of mortars. Silica fume or metakaolinite addition, however, does not show the same increase in strength effects in portland cement pastes, at least for the water-binder ratios used, and the dosages of silica fume or metakaolinite considered in this study. On the basis of the results obtained, it is believed that these improvements are likely to be due to the decrease in thickness of the interfacial zone and the better stress transfer between matrix and aggregate particles.

9 Acknowledgements

The work presented in this article was initiated by Prof. dr. ir. Y. M. de Haan, Head of the Materials Science Group and carried out under the supervision of Prof. dr. J. M. J. M. Bijen, professor of Materials Science Group, Faculty of Civil Engineering. I am very grateful to these two professors for their co-operation. I wish also to express my gratitude to all the members of the Materials Science Group of the Mechanics and Structures Department, Faculty of Civil Engineering who in one way or another contributed to the success of this project, to Dr. Rob Polder of TNO Building and Construction Research, Department of Building Technology, for reviewing the entire manuscript, and to the editorial board of HERON for accepting this work for publication.

10 Notations and symbols

a	aggregate
a/c	aggregate-cement ratio
a/s	aggregate-binder (solids) ratio
AFt	ettringite: $Ca_6Al_2(SO_4)_3(OH)_2 \cdot 25H_2O$
B.E.T. value	specific surface measured with the apparatus of Brunauer, Emmett and Teller (Nitrogen adsorption technique)
Blaine fineness	specific surface measured with the Blaine apparatus (via the air flow through standard compacted powder)
c	cement
C_a	concentration of solution A (m moles/liter)
C_b	concentration of solution B (m moles/liter)
CH	calcium hydroxide, $Ca(OH)_2$
C_3A	tricalcium aluminate: $3CaO \cdot Al_2O_3$
C_4AF	tetracalcium aluminoferrite: $4CaO \cdot Al_2O_3 \cdot Fe_2O_3$
C_2S	dicalcium silicate: $2CaO \cdot SiO_2$
C_3S	tricalcium silicate: $3CaO \cdot SiO_2$
C–S–H gel	calcium-silica-hydrate (amorphous or semi-crystalline of varying stoichiometries)
C/S	CaO/SiO_2 molar ratio
Class F fly ash	fly ash with a low calcium content (originating from combustion of bituminous coal)
δ	thickness of the interfacial zone (μm)
D_i	diffusion coefficient (m^2s^{-1})
EDAX	energy dispersive X-ray analyzer
EPMA	electron probe micro-analysis
E_a	static modulus of elasticity of aggregate
E_m	static modulus of elasticity of matrix
f.a.	fly ash
f_c	ultimate compressive strength (MPa)
H_v	microhardness value
I_{CH}	orientation index of $Ca(OH)_2$ crystals
ICP (ICAP)	inductive coupled (argon) plasma spectrometry
L.O.I.	loss on ignition
m/m	mass by mass
MK	metakaolinite
M_{sat}	mass of saturated surface-dried specimen
Mullite	$Al_6Si_2O_{13}$
opc	ordinary portland cement
OPCM	ordinary portland cement mortar
OPCMP	ordinary portland cement "mortar paste"
OPCP	ordinary portland cement paste
pbfc	portland blast furnace slag cement

pfa	pulverised fuel ash
Portlandite	calcium hydroxide, $Ca(OH)_2$
psd	particle size distribution
R.H.	relative humidity (%)
s	sand; solids; binder; second
s.d.	standard deviation
s.f.; sf	silica fume
SEM	scanning electron microscopy (microscope)
σ_c	compressive strength (MPa)
t	time
V; v	volume
w	water
w/c; w-c	water-cement ratio
w/s; w-s	water-binder (solids) ratio
XRD	X-ray diffractometry (diffractometer)

11 References

1. Mindess, S. (1988), Bonding in cementitious composites: How important is it. In Proceedings Materials Research Symposium (Edited by S. Mindess and S. Shah), Vol. 114, pp. 3–10.
2. Farran, J. (1956), Contribution mineralogique a l'etude de l'adherence entre les constituants hydrates des ciments et les materiaux enrobes. Revue des Materiaux Construction et de Travaux Publics, pp. 155–172.
3. Buck, A. D. and Dolch, W. L. (1966), Investigation of a reaction involving non-dolomitic limestone aggregate in concrete. Journal American Concrete Institute, Vol. 63, No. 7, pp. 755–763.
4. Suzuki, M. and Mizukami, K. (1975), Bond strength between cement paste and aggregate. In Proceedings 29th General Meeting of the Cement Association of Japan, pp. 94–96.
5. Suzuki, M. and Mizukama, K. (1976), Bond strength between cement paste and aggregates. In Proceedings 30th General Meeting of the Cement Association of Japan, pp. 211–213.
6. Hadley, D. (1972), The nature of the paste-aggregate interface. Ph.D. Thesis, Purdue University. 173 p.
7. Barnes, B. D., Diamond, S. and Dolch, W. L. (1978), The contact zone between portland cement paste and glass "aggregate" surfaces. Cement and Concrete Research, Vol. 8, pp. 233–244.
8. Barnes, B. D., Diamond, S. and Dolch, W. L. (1979), Micromorphology of the interfacial zone around aggregates in portland cement mortar. Journal of the American Ceramic Society, Vol. 62, No. 1–2, pp. 21–24.
9. Grandet, J. and Ollivier, J. P. (1980), Nouvelle methode dmetude des interfaces ciment-granulats. In Proceedings 7th International Congress on the Chemistry of Cements, Paris, Vol. III, pp. VII 85–89.
10. Monteiro, P. J. M., Maso, J. C. and Ollivier, J. P. (1985), The aggregate-mortar interface. Cement and Concrete Research, Vol. 15, pp. 953–958.
11. Detwiler, R. J., Monteiro, P. J. M., Wenk, H. R. and Zhong, Z. (1988), The texture of calcium hydroxide near the cement paste-aggregate interface. Cement and Concrete Research, Vol. 18, pp. 823–829.
12. Jia, W. (1988), Mechanism of orientation of $Ca(OH)_2$ crystals in interface layer between paste and aggregate in systems containing silica fume. In Proceedings Materials Research Symposium (Edited by S. Mindess and S. Shah), Vol. 114, pp. 127–132.
13. Diamond, S. (1987), Cement paste microstructure in concrete. In Proceedings Materials Research Symposium (Edited by L. J. Struble and P. W. Brown), Vol. 85, pp. 21–31.
14. Zimbelmann, R. (1978), The problem of increasing the strength of concrete. Betonwerk + Fertigteil-Technik, Heft 2, pp. 89–96, 1978.

15. Conjeaud, M., Lelong, B. and Cariou, B. (1980), Bond between portland cement paste and native aggregates. In Proceedings 7th International Congress on the Chemistry of Cements, Paris, Vol. III, pp. VII 6-11.
16. Farran, J, Javelas, R., Maso, J. C. and Perrin, B. (1972), Existence d'une aureole de la transition entre les granulats d'un mortier, ou d'un beton, et la masse de la pate de ciment hydrate. Consequences sur les proprietes mecaniques. Concrete Research and Academic Scientific Series D. 275, pp. 1467-1469.
17. Scrivener, K. L. and Pratt, P. L. (1986), A preliminary study of the microstructure of the cement-sand bond in mortars. In Proceedings 8th Internatioinal Congress on the Chemistry of Cement, Rio de Janeiro, Vol. III, pp. 466-471.
18. Scrivener, K. L., Bentur, A. and Pratt, P. L. (1988), Quantitative characterization of the transition zone in high strength concretes. Advances in Cement Research, Vol. 1, No. 4, pp. 230-237.
19. Scrivener, K. L. and Gartner, E. M. (1988), The characterization and quantification of cement and concrete microstructures. In Proceedings Materials Research Society Symposium (Edited by S. Mindess and S. P. Shah), Vol. 114, pp. 77-85.
20. Scrivener, K. L., Crumble, A. K. and Pratt, P. L. (1988), A study of the interfacial region between cement paste and aggregatee in concrete. In Proceedings Materials Research Society Symposium (Edited by S. Mindess and S. P. Shah), Vol. 114, pp. 87-88.
21. Struble, L. (1988), Microstructure and fracture at the cement paste-aggregate interface. In Proceedings Materials Research Society Symposium, (Edited by S. Mindess and S. Shah), Vol. 114, pp. 11-20.
22. Grandet, J. and Ollivier, J. P. (1980), Etude de la formation du monocarboaluminate de calcium hydrate au contact d'un granulat calcaire dans une pate de ciment portland. Cement and Concrete Research, Vol. 10, pp. 759-770.
23. Monteiro, P. J. M. and Mehta, P. K. (1985), Ettringite formation on the aggregate-cement paste interface. Cement and Concrete Research, Vol. 15, pp. 378-380.
24. Yuan, C. Z. and Guo, W. J. (1988), Effect of bond strength between aggregate and cement paste on the mechanical behaviour of concrete. In Proceedings Materials Research Society Symposium (Edited by S. Mindess and S. Shah), Vol. 114, pp. 41-47.
25. Mehta, P. K. (1986), Concrete: Structure, Properties, and Materials. Prentice-Hall, Inc. pp. 450.
26. Yuan, C. Z. and Odler, I. (1987), The interfacial zone between marble and tricalcium silicate. Cement and Concrete Research, Vol. 17, pp. 784-792.
27. Massazza, F. and Costa, U. (1986), Bond: Paste-aggregate, paste-reinforcement and paste-fibres. In Proceedings 8th International Congress on the Chemistry of Cement, Rio de Janeiro, Vol. I, pp. 158-180.
28. Cussino, L. and Pintor, G. (1972), An investigation into the different behaviour of silicic and calcareous aggregates in mixes with regard to the mineralogical composition of cement. Il Cemento, Vol. 4, pp. 255-268.
29. Cussino, L., Murat, M. and Negro, A. (1976), Chemical and physical study about the bond between cement and calcareous aggregates in mortars. Il Cemento, Vol. 73, No. 2, pp. 77-90.
30. Zimbelmann, R. (1985), A contribution to the problem of cement-aggregate bond. Cement and Concrete Research, Vol. 15, pp. 801-808.
31. Monteiro, P. J. M. and Mehta, P. K. (1986), Improvement of the aggregate-cement paste transition zone by grain refinement of hydration products. In Proceedings 8th International Congress on the Chemistry of Cement, Rio de Janeiro, Vol. III, pp. 433-437.
32. Scholer, C. F. (1967), The role of the mortar-aggregate bond in the strength of concrete. Highway Research Record, Vol. 210, pp. 108-117.
33. Tognon, G. P. and Cangiano, S. (1980), Interface phenomena and durability of concrete. In Proceedings 7th International Congress on the Chemistry of Cement, Paris, Vol. III, pp. VII 133-VII 138.
34. Kayyali, O. A. (1987), Porosity of concrete in relation to the nature of the paste-aggregate interface, Materials and Structures, Vol. 20, pp. 19-26.

35. Maso, J. C. (1980), The bond between aggregates and hydrated cement paste. In Proceedings 7th International Congress on the Chemistry of Cements, Paris, Vol. I, pp. VII 1-15.
36. Lyubimova, T. Yu. and Pinus, E. R. (1962), Crystallization structure in the contact zone between aggregate and cement in concrete. Colloid Journal, USSR, Vol. 24, No. 5, pp. 491-498.
37. Yuji, W. (1988), The effect of bond characteristics between steel slag fine aggregates and cement paste on mechanical properties of concrete and mortar. In Proceedings, Materials Research Society Symposium (Edited by S. Mindess and S. Shah), pp. 49-54.
38. Mehta, P. K. and Monteiro, P. J. M. (1988), Effect of aggregate, cement, and mineral admixtures on the microstructure of the transition zone. In Proceedings Materials Research Society Symposium (Edited by S. Mindess and S. P. Shah), Vol. 114, pp. 65-75.
39. Hsu, T. T. C. and Slate, F. O. (1963), Tensile bond strength between aggregate and cement paste or mortar. Journal of American Concrete Institute, Vol. 60, No. 4, pp. 465-486.
40. Shah, S. P. and Slate, F. O. (1968), Internal microcracking, mortar-aggregate bond, and stress-strain curve of concrete. In Proceedings Structure of Concrete (Edited by Brooks, A. E. and Newman, K.), pp. 82-92.
41. Hsu, T. T. C, Slate, F. O., Stuurman, G. M. and Winter, G. (1963), Micro-cracking of concrete and the shape of the stress-strain curve. Journal of American Concrete Institute, Vol. 60, No. 3, pp. 209-224.
42. Slate, F. O. and Olsefski, S. (1963), X-rays for study of internal structure and micro-cracking of concrete. Journal of American Concrete Institute, Vol. 60, No. 5, pp. 575-588.
43. Alexander, K. M., Wardlaw, J. and Gilbert, D. J. (1968), Aggregate-cement bond, cement paste strength and the strength of concrete. In Proceedings Structure of Concrete (Edited by A. E. Brooks and K. Newman), pp. 59-81.
44. Marchese, B. (1983), Morphology and composition of twin fracture surfaces of a crack in portland cement paste. Cement and Concrete Research, Vol. 13, pp. 435-440.
45. Fagerlund, G. (1973), Strength and porosity of concrete. In Proceedings of the International Symposium on Pore Structure and Properties of Materials, RILEM/IUPAC, Prague. pp. D51-D73.
46. Perry, C. and Gillott, J. E. (1977), The influence of mortar-aggregate bond strength on the behaviour of concrete in uniaxial compression. Cement and Concrete Research, Vol. 7, pp. 553-564.
47. Neville, A. M. (1981), Properties of concrete. Longman Scientific and Technical, 3rd Edition, 779p.
48. Brandt, I., Jensen, A. D. and Strunge, H. (1983), Microcracking in concrete: Method to quantify micro-cracks on thin sections. Report - Building Technology, Technological Institute, Taastrup, Denmark, 10p.
49. Glucklick, J. (1968), The effect of microcracking in time-dependent deformations and the longterm strength of concrete. In Proceedings International Conference on the Structure of Concrete (Cement and Concrete Association), London, pp. 82-92.
50. Regourd, M. (1985), Microstructure of high strength cement paste systems. In Proceedings Materials Research Society Symposium (Edited by J. F. Young), Vol. 42, pp. 3-17.
51. Bentur, A., Goldman, A. and Cohen, M. D. (1988), The contribution of the transition zone to the strength of high quality silica fume concretes. In Proceedings, Materials Research Society Symposium (Edited by S. Mindess and S. Shah), pp. 97-103.
52. Detwiler, R. J. and Mehta, P. K. (1989), Chemical and physical effects of silica fume on the mechanical behaviour of concrete. American Concrete Institute Materials Journal, No. 86-M60, pp. 609-614.
53. Mindess, S. (1986), Significance to concrete performance of interfaces and bond: Challenges of the future. In Proceedings 8th International Congress on the Chemistry of Cement, Rio de Janeiro, Vol. I, pp. 151-157.
54. Keru, W. and Jianhua, Z. (1988), The influence of the matrix-aggregate bond on the strength and brittleness of concrete. In Proceedings Materials Research Society Symposium (Edited by S. Mindess and S. Shah), pp. 29-34.

55. SARKAR, S. L. and AITCIN, P-C. (1987), Comparative study of the microstructure of normal and very high-strength concretes. Cement, Concrete and Aggregates, CCAGDP, Vol. 9, No. 2, pp. 57–64.
56. GOLDMAN, A. and BENTUR, A. (1989), Bond effects in high strength silica-fume concretes. American Concrete Institute Materials Journal, Vol. 86, No. 5, pp. 440–447.
57. MINDESS, S. and DIAMOND, S. (1982), A device for direct observation of cracking of cement paste or mortar under compressive loading within a scanning electron microscope. Cement and Concrete Research, Vol. 12, pp. 569–576.
58. MINDESS, S. and DIAMOND, S. (1982), The cracking and fracture of mortar. Materiaux et Constructions (Paris), Vol. 15, pp. 107–113.
59. BENTUR, A. and MINDESS, S. (1986), The effect of concrete strength on crack patterns. Cement and Concrete Research, Vol. 16, pp. 59–66.
60. ODLER, I. and ZURZ, A. (1988), Structure and bond strength of cement-aggregate interfaces. Materials Research Society Symposium (Edited by S. Mindess and S. Shah), pp. 21–27.
61. WAKELY, L. D. and ROY, D. M. (1982), A method of testing the permeability between grout and rock. Cement and Concrete Research, Vol. 12, pp. 533–534.
62. MALEK, R. I. A. and ROY, D. M. (1988), The permeability of chloride ions in fly ash-cement pastes, mortars and concrete. In Proceedings Materials Research Society Symposium (Edited by S. Mindess and S. Sha), Vol. 114, pp. 325–334.
63. VALENTA, O. (1961), The significance of the aggregate-cement bond for durability of concrete. In Proceedings International Symposium on Durability of Concrete, RILEM, Prague, Preliminary Report, pp. 53–87.
64. VALENTA, O. (1969), Durability of Concrete. In Proceedings 5th International Symposium on the Chemistry of Cement, Tokyo, Vol. III, pp. 193–225.
65. XIE, P. and TANG, M. (1988), Relationship between characteristics portland cement paste-aggregate interface and electrical conductivity of mortar. Journal of the Chinese Silicate Society, Vol. 16, No. 2, pp. 97–103.
66. NORTON, P. T. and PLETTA, D. H. (1931), The permeability of gravel concrete. Journal of the American Concrete Institute, Vol. 27, pp. 1093–1132.
67. NYAME, B. K. (1985), Permeability of normal and lightweight mortars. Magazine of Concrete Research, Vol. 37, No. 130, pp. 44–48.
68. TOY, H. C. (1924), The permeability of concrete. London Institute of Civil Engineers (ICI Selected Engineering Paper), No. 20.
69. MURATA, J. (1965), Studies on the permeability of concrete. RILEM Bulletin, New Series, No. 29, pp. 47.
70. BRACS, G., BALINT, E. and ORCHARD, D. F. (1970), Use of electrical resistance probes in tracing moisture permeation through concrete. Journal of the American Concrete Institute, Vol. 67, No. 8, pp. 642–648.
71. DETWILER R. J. and MEHTA, P. K. (1989), Chemical and physical effects of condensed silica fume in concrete. In Proceedings 3rd Canmet/ACI International Conference on Fly ash, silica fume, slag and natural pozzolans in concrete (Edited by M. Alasali), Trondheim, Norway, (Suplementary Papers).
72. CHENG-YI, H. and FELDMAN, R. F. (1985), Influence of silica fume on the microstructural development in cement mortars. Cement and Concrete Research, Vol. 15, pp. 285–294.
73. SARKAR, S. AITCIN, P-C. and DJELLOULI, H. (1990), Synergistic roles of slag and silica fume in very high-strength concrete. Cement, Concrete and Aggregates, CCAGDP, Vol. 12, No. 1, pp. 32–37.
74. DARWIN, D., ZHENJIA, S. and HARSH, S. (1988), Silica fume, bond strength, and the compressive strength of mortar. In Proceedings Materials Research Society Symposium, Vol. 114 (Edited by S. Mindess and S. Shah), pp. 105–110.
75. DETWILER, R. KRISHNAN, K. and MEHTA, P. (1986), Effect of blast furnace slag on the transition zone in concrete. In Proceedings Bryan and Katharine Mather International Symposium on Durability of Concrete, Atlanta, ACI SP 100-6, Vol. 1, pp. 63–72.

76. Saito, M. and Kawamura, M. (1989), Effect of fly ash and slag on the interfacial zone between cement and aggregate. In Proceedings 3rd Canmet/ACI International Conference on Fly ash, silica fume, slag and natural pozzolans in concrete (Edited by M. Alasali), Trondheim, Norway, SP114-32, pp. 669–688.
77. Gjorv, O. E., Monteiro, P. J. M. and Mehta, P. K. (1990), Effect of condensed silica fume on the steel-concrete bond. Journal of American Concrete Institute, Vol. 87, No. 6, pp. 573–580.
78. Xueqan, W., Sufen H., Qinghan, B. and Mingshu, T. (1986), Effect of pretreatment of aggregate surface on the properties of concrete. In Proceedings 8th International Congress on the Chemistry of Cement, Rio de Janeiro, Vol. III, pp. 433–437.
79. Xueqan, W., Dongxu L., Xiun, W. and Minshu, T. (1988), Modification of the interfacial zone between aggregate and cement paste. In Proceedings Materials Research Society Symposium (Edited by S. Mindess and S. Shah), Vol. 114, pp. 35–40.
80. Su. Z. and Bijen, J. M. J. M. (1990), The effect of polymer dispersions on the interface between cement paste and aggregates. In Proceedings 6th International Congress on Polymers in Concrete, Beijin, China (Edited by H. Yiun-Yuan, W. Keru, C. Zhiyuan), pp. 474–481.
81. Su, Z., Bijen, J. and Larbi, J. A. (1991), The influence of polymer modification on the adhesion strength of pastes to aggregates. Cement and Concrete Research, Vol. 21, pp. 169–178.
82. Franke, V. B. (1941), Bestimmung von calcium oxyd und calciumhydroxyd neben wasserfreien und allgemeine, Band 247.
83. Larbi, J. A. (1991), The Cement Paste-Aggregate Interfacial Zone in Concrete. Ph.D. Thesis, Delft Technical University, 127 p.
84. Kondo, R., Satake, M. and Ushiyama, H. (1974), Diffusion of various ions in hardened portland cement. In Proceedings 28th General Meeting of the Cement Association of Japan, Tokyo, No. 28.
85. Page, C. L., Short, N. R. and ElTerras, A. (1981), Diffusion of chloride ions in hardened cement pastes. Cement and Concrete Research, Vol. 11, pp. 395–406.
86. Short, N. R. and Page, C. L. (1982), The diffusion of chloride ions through portland and blended cement pastes. Silicate Industriels, No. 10, pp. 237–240.
87. Dhir, R. K., Jones, M. R. Ahmed, H. E. H. and Seneviratne, A. M. G. (1990), Rapid estimation of chloride diffusion coefficient in concrete. Magazine of Concrete Research, Vol. 42, No. 152, pp. 177–185.
88. Buenfeld, N. R. and Newman J. B. (1987), Examination of three methods for studying ion diffusion in cement pastes, mortars and concrete. Materials and Structures, Vol. 20, pp. 3–10.
89. Feldman, R. F. (1986), The effect of sand-cement ratio and silica fume on the microstructure of mortar. Cement and Concrete Research, Vol. 16, pp. 31–39.
90. Uchikawa, H., Uchida, S. and Hanehara, S. (1989), Relationship between structure and penetrability of Na ion in hardened blended cement paste, mortar and concrete. In Proceedings 8th International Conference on Alkali-Aggregate Reaction, Kyoto, pp. 121–128.
91. Collepardi, M., Marcialis, A. and Turriziani, R. (1972), Penetration of chloride y ions into cement paste and concretes. Journal of American Ceramic Society, Vol. 55, No. 10, pp. 534–535.
92. Sturrup, V. R., Hooton, R. D. and Clendenning, T. G. (1983), Durability of fly ash concrete. American Concrete Institute (ACI), SP-79, Vol. 1, pp. 71–86.
93. Powers, T. C. and Brownyard, T. L. (1947), Studies of physical properties of hardened portland cement paste. Journal of American Concrete Institute, Vol. 43, No. 7, pp. 101–132, 249–336, 469–504, 549–602, 669–712, 815–880, 933–992.